

UCSF

UC San Francisco Electronic Theses and Dissertations

Title

Nondestructive assessment of white spot lesions using near infrared imaging

Permalink

<https://escholarship.org/uc/item/1xf9j9ds>

Author

Wu, Jennifer

Publication Date

2008

Peer reviewed|Thesis/dissertation

**Nondestructive Assessment of White Spot
Lesions Using Near Infrared Imaging**

by

Jennifer Wu, D.D.S.

THESIS

Submitted in partial satisfaction of the requirements for the degree of

MASTERS OF SCIENCE

in

ORAL AND CRANIOFACIAL SCIENCES

in the

GRADUATE DIVISION

of the

UNIVERSITY OF CALIFORNIA

San Francisco



Date

University Librarian

ACKNOWLEDGEMENTS

I would like to thank my committee members Dr. Daniel Fried, Dr. Arthur Miller, and Dr. Michal Staninec for their support and guidance. I would like to thank Dr. Fried for being a great mentor. He made it easier for me to understand my project and was always willing to answer any questions. I would like to thank Dr. Miller for pushing me to work hard and finish in a timely manner. His encouragement and our quarterly presentations, I would still be working on my project. I would like to thank Dr. Staninec for guidance and feedback with the project.

ABSTRACT

PURPOSE: This study used near-infrared imaging (NIR) at 1310 nm to acquire high contrast images of early surface enamel demineralization, (i.e. “white spot lesions”). The specific aims were 1) to test the hypothesis that we can measure significant differences in optical contrast at 1310 nm between sound and artificially demineralized enamel on the buccal and occlusal surfaces; and 2) to test the hypothesis that NIR imaging manifests greater contrast than other promising methods, including qualitative light fluorescence (QLF) and visible light reflectance with cross-polarization.

METHODS: Fifteen human molar samples were used in this *in vitro* study. Teeth were painted with a clear varnish, leaving a 2x2 window on the buccal and occlusal surfaces for demineralization. Teeth were exposed for 48 hours to demineralization solution at pH 4.5. Teeth were imaged with the following methods: NIR-Transillumination with cross polarization, NIR reflectance imaging with cross polarization; Visible light reflectance imaging with cross polarization, NIR imaging from occlusal aspect, NIR imaging with a fiber optic probe.

RESULTS: NIR reflectance imaging with cross polarization had the highest image contrast. This was the only method that provided significantly higher contrast than the visible light reflectance with cross-polarization images.

CONCLUSION: NIR imaging has considerable potential for imaging of early surface demineralization of sound enamel. NIR reflectance imaging with cross polarization can be a useful tool for non-destructive routine monitoring of white spot lesions around orthodontic brackets during orthodontic treatment.

TABLE OF CONTENTS

ACKNOWLEDGEMENTS	III
ABSTRACT	IV
TABLE OF CONTENTS	V
LIST OF TABLES	VIII
LIST OF FIGURES	IX
INTRODUCTION	1
Demineralization around brackets	1
Optical properties of teeth	3
Visible Light	4
Quantitative Light Fluorescence (QLF)	5
Near Infrared Imaging	7
Polarization sensitivity Optical Coherence Tomography (PS-OCT)	9
Purpose	10
Specific Aims	10
MATERIALS AND METHODS	11
A. Sample Preparation	11
1. Sample Acquisition and Mounting	11
2. Fiducial Marking	11
3. Enamel Varnish Application	12
B. Demineralization Challenge	12
C. Methods of Imaging	13
NIR- Transillumination	13

NIR- Reflectance Imaging with Polarization	14
Near Infrared Single Fiber Probe	15
Qualitative Light Fluorescence	17
Visible Light Reflectance with Cross Polarization	18
D. Methods of Image Analysis	19
PS-OCT (Polarization Sensitive – Optical Coherence Tomography)	22
1. PS-OCT Imaging	22
3. PS-OCT Line Profiles	22
RESULTS	25
A. Buccal Images	25
B. Occlusal Images	29
DISCUSSION	33
CONCLUSION	38
APPENDICES	44
Appendix A: Pilot Study	45
Appendix B: Buccal images	50
Tooth 1	51
Tooth 2	52
Tooth 3	53
Tooth 4	54
Tooth 5	55
Tooth 6	56
Tooth 7	57
Tooth 8	58
Tooth 9	59
Tooth 10	60
Tooth 11	61
Tooth 12	62
Tooth 13	63
Tooth 14	64
Tooth 15	65

Appendix C: Occlusal Images

	66
Tooth 1	67
Tooth 2	68
Tooth 3	69
Tooth 4	70
Tooth 5	71
Tooth 6	72
Tooth 7	73
Tooth 8	74
Tooth 9	75
Tooth 10	76
Tooth 11	77
Tooth 12	78
Tooth 13	79
Tooth 14	80
Tooth 15	81

List of Tables

Table 1 Buccal image contrast values of the five different imaging methods for all 15 teeth. A higher number depicts a larger contrast. A negative number occurs when the lesion appears lighter when it should appear darker than the sound enamel	25
Table 2 Buccal image contrast means and standard deviation for the 5 different imaging methods.....	26
Table 3 Results of ANOVA followed by the Tukey-Kramer post-hoc multiple comparison test.	27
Table 4 Buccal OCT values for all 15 teeth. A high number in the lesion and a low number in the sound shows that there is demineralization in areas of interest.....	28
Table 5 Image contrast values for the 5 different occlusal methods. A higher number represents a greater contrast between sound and demineralized enamel.....	29
Table 6 The mean and standard deviations for the 4 different occlusal imaging methods.	30
Table 7 ANOVA followed by Tukey Kramer post-hoc results with P values	30
Table 8 Occlusal OCT Reflectivity Values	32

List of Figures

Figure 1. Plot of attenuation coefficient of dental enamel (filled circles) and the absorption coefficient of water (open circles) versus wavelength(Fried, 1995).....	8
Figure 2 An example of a tooth with fiducial markings, creating a 2x2 window on the buccal and occlusal surface	11
Figure 3 An example of an image of both buccal and occlusal surfaces of a tooth after 48 hours in demineralization solution. The demineralized regions appear white and are contained in the 2x2 window.....	13
Figure 4 NIR Transillumination setup for buccal lesions. The NIR light comes behind the tooth and travels through cross polarizers before reaching and illuminating the tooth. The InGaAs focal plane array is in front of the tooth and takes an image of the buccal surface of the tooth.....	13
Figure 5. Buccal NIR transillumination image taken with the setup shown in figure 4. The transparency of the enamel in the NIR is apparent. The demineralized region within the 2x2 window appears darker than the surrounding enamel.	14
Figure 6 NIR Transillumination occlusal imaging setup. The NIR light comes from behind the tooth and enters the tooth just above the DEJ and is scattered by the dentin. The camera is positioned directly above the occlusal surface of the tooth.	15
Figure 7 Example of Transillumination-NIR occlusal image. The demineralized region appears darker than the surrounding sound enamel.....	15
Figure 8 NIR reflectance imaging with cross polarization setup for buccal and occlusal lesions. 8A) The NIR light comes into the tooth at an angle, and the image is captured with the camera aimed at the buccal surface. 8B) The occlusal image is obtained with the same setup. The tooth is turned on its side so the occlusal surface is positioned in front of the camera.	16
Figure 9 Buccal and occlusal NIR reflective with polarization images. The demineralized region appears lighter than the surrounding sound enamel.	16
Figure 10 NIR Single Fiber Probe - NIR with polarization . The probe directs the NIR onto the occlusal surface of the tooth. Crossed polarizers were used to block out unwanted light. The image was taken from the buccal surface of the tooth.....	17
Figure 11 Buccal single fiber probe – NIR image. The demineralized region in the 2x2 window appears darker than the surrounding sound enamel.....	18
Figure 12 Buccal and Occlusal QLF image. The demineralized region appears darker than the surrounding sound enamel.	18
Figure 13 Buccal and occlusal visible with cross polarziation images. The demineralized region appears lighter than the surrounding sound enamel.	19
Figure 14 Example of a line profile taken through the image. The two blue lines show the boundaries of the position of the line profile, which is centered half way through the bottom half of the demineralized area.	20
Figure 15. This graft is the line profile from the image in Figure 14. The x-axis represents the distance across the tooth. The Y-axis represents the reflectivity along the position. The red line represents the line profile, and the blue line represents the integration of the line profile.	21

Figure 16 Image of a line profile taken through the center of the demineralized region. The y-axis represents the axial distance into the tooth. The x-axis represents the distance along the tooth surface. The lesion area is shown between the two red lines.....23

Figure 17 Integrated line profile with markers at the surface and a point 400 um into the tooth, along the x-axis in an area with a lesion. The red line represents the line profile. The blue line is the integration of the line profile. The background reflectivity is zeroed.24

Figure 18 Buccal image contrast means with standard deviation. The error bars represent standard deviations. Bars with the same color are not significantly different from each other, $P>0.05$26

Figure 19 Occlusal image contrast means with standard deviation. The error bars represent standard deviations. Bars with the same color are not significantly different from each other, $P>0.05$31

Introduction

Demineralization

Dental caries occurs when there is an imbalance between the rate of demineralization and remineralization. The organic acids produced by the bacteria in the plaque diffuse through the porous enamel of the tooth and dissolve the mineral crystals as they diffuse into the tooth (Featherstone, 2000). If this decay process is not stopped, the demineralization can spread through the enamel and reach the dentin. Once it reaches the dentin, it rapidly accelerates due to the higher solubility and permeability of dentin. As the lesion spreads underneath the dentin, it results in cavitation and loss of integrity. Early diagnosis of demineralization allows for nondestructive preventive measures, which can save tooth structure, time and money.

Demineralization around brackets

Decalcification around orthodontic brackets is a serious complication of orthodontic treatment because it can interfere with the esthetic benefits of braces. It has been reported in as many as 50% of patients treated with fixed appliances.(Travess et al., 2004) Other studies have reported a prevalence of demineralization ranging from 2 to 96 per cent.(Mitchell, 1992) Studies have shown an increased incidence of carious lesions on facial and lingual surfaces during orthodontic treatment, and can be found in as little time as one month.(Gorelick et al., 1982) These lesions have been shown to occur on the buccal surfaces of teeth, an area which normally shows a low level of caries prevalence.(Ogaard et al., 1988) Another study found that after 5 years of orthodontic treatment, orthodontic patients had a significantly higher incidence of white spot lesions

compared to a control group.(Ogaard, 1989) Not only are these white spot lesions unaesthetic and irreversible, it can lead to early discontinuation of treatment, and thus a non-ideal orthodontic result.

Decalcification is a result of a patient's inability to maintain proper oral hygiene while the fixed appliances are in place. As a result, plaque accumulates around the brackets. Enamel demineralization is often associated with fixed orthodontic therapy due to the high and continuous cariogenic challenge in the plaque developed around brackets and bands.(Ogaard et al., 1988)

Due to the loss of translucency in the enamel in these areas, the demineralization is often referred to as white spot lesions. The resulting lesion is not cavitated, but appears as a rough surface.(Featherstone, 1985) The initial appearance appears chalky white. If mineral loss continues, a subsurface lesion will result.(Featherstone, 1985)

If these lesions are detected early, they can be arrested or even reversed by many non-invasive methods. A clinician can prescribe antibacterial rinses, fluoride treatments, and dietary changes in attempt to naturally remineralize the decay before it becomes irreversible.(Featherstone, 1999) A systematic review found that daily sodium fluoride mouth rinse will reduce the occurrence and severity of white spot lesions during orthodontic treatment, although the best method is still unclear.(Benson et al., 2005a)

Longitudinal monitoring of the decalcification is necessary for determining the success of the therapy for arresting or reversing early dental decay. This will allow the clinician to determine whether or not treatment for arresting the decalcification is successful. Conventional therapies, including a dental probe and x-rays do not precisely measure the depth of early decay. Due to ionizing radiation exposure, conventional x-

rays are not indicated for regular monitoring of the lesion. X-rays are appropriate for large, cavitated lesions, but do not have sufficient sensitivity to detect early, noncavitating lesions. Therefore, a new nondestructive method to monitor decalcification is needed.

Optical properties of teeth

Dental enamel is composed of an ordered array of inorganic apatite-like crystals surrounded by a protein/lipid/water matrix. Human enamel consists of hydroxyapatite crystals that form enamel rods which are arranged perpendicular to the tooth surface. The crystals are approximately 30 – 40 nm in diameter and can be as long as 10 μm . These crystals are clustered in rods which are perpendicular to the tooth surface. As a result of the nature of dental enamel, the scattering distributions are anisotropic and depend on the tissue orientation relative to the irradiating light source.(D. Fried, 1995) During demineralization of enamel, dissolution of the mineral phase creates pores that highly scatter light.(Jones, 2006) The pores in enamel are formed due to demineralization when caries are present.(Featherstone, 1985). These pores cause an increase in light scattering.

Dentin is composed of 30% organic material (collagen fibrils), 20% water, and 50% inorganic materials (carbonated hydroxyapatite crystals). The dentinal tubules that make up dentin radiate from the pulp to the DEJ in an S-shaped fashion. These tubules scatter the light. This light scattering in dentin, which is greater than enamel, results in its yellow appearance, compared to the translucent color of dental enamel.(Feldchtein FI, 1998) The tubules are oriented almost perpendicular to the propagation direction at the DEJ. Thus, the backscattering signal is strong with increasing depth as the tubule density changes.(Wang XJ, 1999)

The optical properties of tooth enamel and dentin change as a result of demineralization. Thus, caries detection schemes that exploit these changes have considerable promise for early detection of carious lesions. (Angmar-Mansson and ten Bosch, 1987)

Visible Light

Clinical photographs are a way of recording the appearance of dental enamel before and after orthodontic treatment. White spot lesions can be measured reliably from photographs, and can be used as a clinical record for assessment of white spot lesions. (Kanthathas et al., 2005; Willmot et al., 2000) A recent study has found that white spots can be assessed accurately and reproducibly from digital images as images captured from a photographic slide. (Benson et al., 2005b) Clinically, it can be difficult to distinguish a white spot lesion from a developmental lesion, as both appear white. Post-orthodontic white spot lesions are more likely to have an irregular shape compared to developmental lesions, with the shape often reflecting the margins of the bracket. (Kanthathas et al., 2005) Developmental lesions have also been shown to have a higher luminance intensity proportionality, and therefore, appear whiter compared to the surrounding enamel. (Kanthathas et al., 2005) However, using this approach relies on subjective assessments of what is sound and demineralized enamel.

Reflections of light from the camera flash may also attribute to failure to identify white lesions or over-estimate the area of the white spot lesion. (Willmot et al., 2000) Light from a camera flash can be reduced using cross polarization. By placing a polarizing filter over the lens, the light can be prevented from reaching the camera. Cross

polarization has been shown to reduce reflections from flash and improve clinical assessments of photographs.(Benson P, 2007)

The main factor that impedes caries detection in the visible range of 400 to 700 nm is light scattering. Light scattering is strong in both the sound enamel and dentin in the visible range, and this obscures light transmission through teeth.(Fried, 1995)

Optical imaging through dental tissues is limited by light scattering, which produces diffuse light that is much stronger than the directly transmitted or “ballistic” light that passes through the tooth without scattering. This prevents imaging of the transmitted light.

Quantitative Light Fluorescence (QLF)

QLF has been the most extensively researched for measuring demineralization on smooth surfaces *in vivo*. Caries can be detected using qualitative light fluorescence because the fluorescence intensity at the site of a lesion is reduced. The fluorescence image of enamel with incipient lesions can be digitized, and the loss of fluorescence in the lesion can be quantified in comparison with the fluorescence intensity level of sound enamel.

In QLF, light exiting the tooth surface is attenuated by light-scattering in the caries lesion. The imaging light is yellow/green fluorescence generated below the tooth surface in sound tissues via excitation with incident blue-green light from the surface.(Bosch, 1999) Part of the mechanism of QLF involves the autofluorescence of sound teeth, which is likely caused by aromatic amino acids in dentin collagen after illumination of high intensity blue light.(Spitzer and Bosch, 1975) Enamel caries can be identified from sound tissue because the demineralized lesion scatters and attenuates the

returning fluorescence signal.(Angmar-Mansson and ten Bosch, 1987) QLF measures a decrease in the returning fluorescence signal and the lesion appears dark from attenuation in the QLF images.

Hafstroem-Bjoerkman et al. established an experimental relationship between the loss of fluorescence intensity, from underlying dentin, and the extent of enamel demineralization.(Hafstrom-Bjorkman et al., 1992) The amount of fluorescence intensity loss has been validated with transverse and longitudinal microradiography in previous studies and has been found to be closely correlated to the mineral loss in the lesion.(Ando *et al.*, 1997; Hafstrom-Bjorkman *et al.*, 1992) An empirical relationship between overall lesion demineralization versus loss of fluorescence, was established which can be used to monitor lesion progression on smooth surfaces.(Lagerweij et al., 1999) Previous studies have found that QLF may be useful for longitudinal monitoring of enamel lesions.(Aljehani *et al.*, 2004; Benson *et al.*, 2003) Unfortunately, QLF cannot readily be applied to occlusal and interproximal lesions, and cannot be used to detect subsurface lesions.(D. Fried, 2002)

Recent studies indicated that QLF is suitable for *in-vivo* monitoring of mineral changes in incipient enamel lesions.(Al-Khateeb et al., 1998; Mattousch et al., 2007) QLF is designed for very early lesions such as those in which the demineralization is localized to the surface.(Eggertsson et al., 1999) Thus, QLF can be an appropriate method for detecting early demineralization around orthodontic brackets.

A study by Pretty et al demonstrated the potential for QLF to longitudinally monitor de- and re-mineralization of enamel adjacent to orthodontic brackets. They also showed a strong positive correlation for quantification of mineral loss.(Pretty et al., 2003)

It has also been shown that in-vivo, QLF was able to detect demineralization before it was visible to the examiner.(Boersma, 2005; Pretty et al., 2003) Another study also concluded that QLF could be used to detect and longitudinally monitor the progression of incipient caries, but discovered that lesion detection may be limited by presence of saliva or plaque and enhanced by staining.(Amaechi and Higham, 2002) QLF has been shown to work *in vivo* for assessing early caries activity.(Meller et al., 2006)

There have not been many studies on the ability of QLF to detect occlusal caries. One reason that QLF cannot be easily applied to non-smooth surfaces is that the change in fluorescence is a measured relative ratio, comparing the loss of fluorescence of caries demineralization to a reference sound area on the tooth. This method implies that the path length of the returning fluorescence signal is comparable, which is impossible to ascertain in the high convoluted occlusal regions.(Jones, 2006) Previous studies have shown that different fluorescence signals from comparable lesions can be produced from variations in total enamel thickness(Ando et al., 2003) and the imaging angle.(Ando et al., 2004)

Near Infrared Imaging

In the NIR region from 780 nm to 1550 nm, the amount of light scattering and absorption in dental hard tissue is weak.(Fried, 1995) Studies have shown that enamel has the highest transparency in the NIR region near 1310nm.(Fried, 2002a) At this wavelength, the attenuation coefficient is only 2 to 3 cm^{-1} , which is a factor of 20 to 30 times lower than in the visible region.(Darling et al., 2006) At longer wavelengths, water absorption increases significantly and reduces the penetration of the NIR light, as shown in Figure 1.

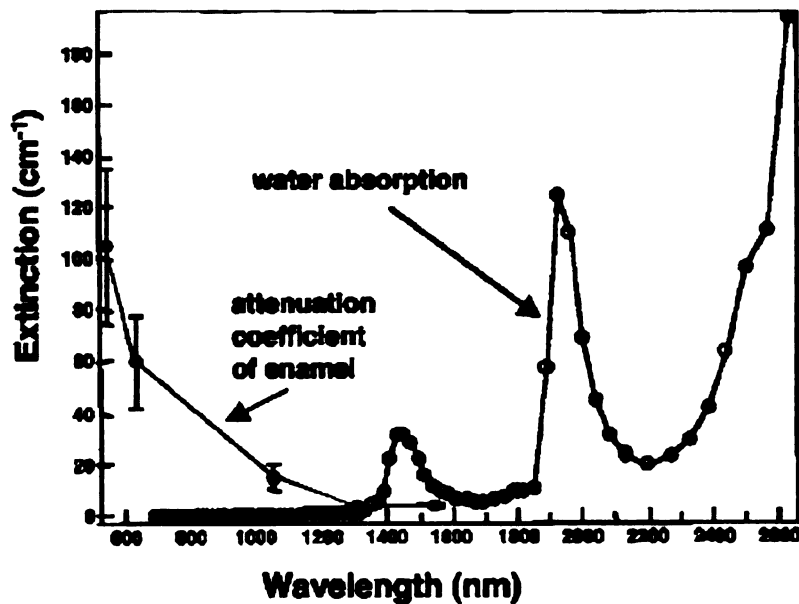


Figure 1. Plot of attenuation coefficient of dental enamel (filled circles) and the absorption coefficient of water (open circles) versus wavelength(Fried, 1995).

The inverse of attenuation coefficient is the mean free path, which is the distance an average photon travels before it is scattered or absorbed. The mean free path is ~3mm for 1310 nm and 1550 nm compared to less than a tenth of a millimeter for wavelengths in the visible range. This is because the magnitude of Rayleigh scattering decreases with increasing wavelengths. Based on scattering alone, attenuation should be lower at 1550 nm than at 1310 nm, however, absorption by water in enamel contributes to attenuation at longer wavelengths. The absorption coefficient of water is low at 1310 nm.(Fried, 2002b)

NIR light at 1310 nm has been shown to be ideally suited for dental caries because of the high contrast between sound and demineralized areas.(Fried et al., 2005) Although the light scattering for sound enamel is low in the NIR, the light scattering in demneralized enamel is high due to the formation of pores on a similar size scale to the

wavelength of the light which acts as Mie scatterers. (Darling et al., 2006) It has also been shown that in the NIR, demineralization can be distinguished from stains, pigmentation, and fluorosis. (Buhler, 2005) NIR light has been shown to be well suited for the detection and imaging of interproximal caries lesions. (Jones, 2003) These investigators have found that optical transillumination is similar to other projection imaging modalities like conventional x-rays, however, the image contrast arises from changes in tissue scattering as opposed to variations in tissue density, and thus, it is a more sensitive method for resolving early caries lesions. (Jones, 2003)

Another study accessed the ability of NIR to image decay on the occlusal surfaces of teeth. The NIR entered the tooth from the buccal surface, and diffused through the highly scattering dentin, providing a uniform back illumination of the enamel of the crowns allowing imaging of the occlusal surface. They were able to show high contrast between sound and demineralized areas. (Buhler, 2005) The demineralization results in attenuation of the light and interferes with imaging within the transparent enamel areas.

Crossed polarizers are used to block out light that does not travel through the birefringent enamel tissue, which is necessary to prevent detector saturation from the illumination, and aid in detecting shallow lesions. (Jones, 2006)

Polarization sensitivity Optical Coherence Tomography (PS-OCT)

PS-OCT is a noninvasive technique for creating cross-sectional images of internal biological structure. The intensity of backscattered light is measured as a function of its axial position (depth) in the tissue. PS-OCT has been shown to provide additional contrast between sound and demineralized tissues. (Baumgartner, 2000; Fried, 2002) Demineralized areas in the tooth cause a large increase in the reflected signal in the fast

axis (perpendicular polarization) due to depolarization from scattering, allowing easier discrimination of caries lesions.(Fried, 2002)

Purpose

The purpose of this study is to use near-infrared imaging at 1310 nm to acquire high contrast images of early surface demineralization of white spot lesions

Specific Aims

The specific aims are to:

- to test the hypothesis that we can measure significant differences in optical contrast at 1310 nm between sound and artificially demineralized enamel on the buccal and occlusal surfaces
- to test the hypothesis that NIR imaging manifests greater contrast than other promising methods, including laser induced fluorescence and visible light reflectance with cross-polarization

Materials and Methods

A. Sample Preparation

1. Sample Acquisition and Mounting

Previous studies have shown that sample sizes of 10-20 have been of sufficient size to detect significant difference in groups. Fifteen teeth with non-carious buccal and occlusal surfaces were selected and sterilized with gamma radiation. Each sample was polished with a 5- μ m aluminum oxide slurry in 5 second intervals for one minute to ensure a homogeneous surface for generating demineralized lesions. Each tooth was mounted in black orthodontic acrylic blocks. Samples were stored in a moist environment of 0.1% thymol to maintain tissue hydration and prevent bacterial growth.

2. Fiducial Marking

A 2x2 mm window was made on both the buccal and occlusal surface of each sample, as shown in Figure 2. The Fiducial markings were created using the TEA CO₂ laser (Impact 2500, GSI Lumonics Rugby, UK) to ablate 50- μ m in depth landmarks into the enamel.



Figure 2 An example of a tooth with fiducial markings, creating a 2x2 window on the buccal and occlusal surface

3. Enamel Varnish Application

The enamel surrounding the 2x2 windows created by the fiducial marking was painted with an acid-resistant clear varnish (Clear, Revlon, New York). This is the first attempt at using clear varnish to prevent demineralization. Previous studies have used red varnish to prevent demineralization. Clear varnish was selected because it does not interfere with imaging, and thus does not need to be removed prior to imaging. A pilot study on bovine enamel blocks demonstrated that the clear varnish does not interfere with imaging in either the visible or NIR region (see appendix A). The varnish was painted around the 2x2 windows to create an area of contrast where the window would have enamel that would be subject to demineralization.

B. Demineralization Challenge

Artificial white spot lesions were created within the 2x2 window using a demineralization regimen, as shown in Figure 3. Each sample was placed in a tube with a 50 ml aliquot of acetate buffer solution containing 2.0 mmol/L calcium, 2.0 mmol/L phosphate, and 0.075 mol/L acetate maintained at pH 4.5 and a temperature of 37°C. The samples were placed in the solution for 48 hours.

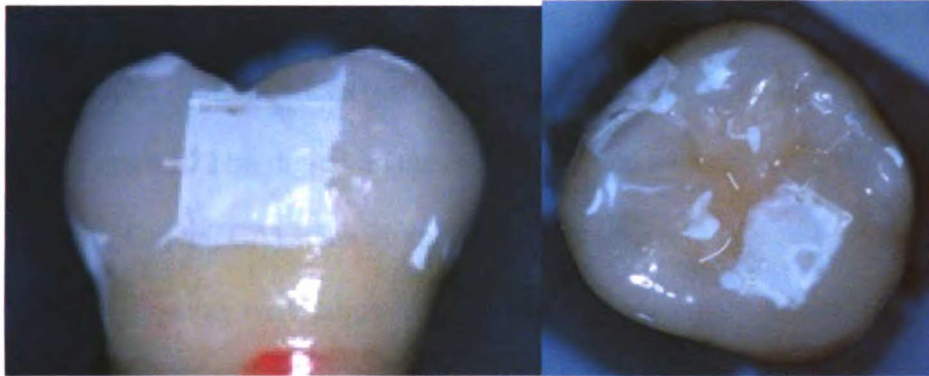


Figure 3 An example of an image of both buccal and occlusal surfaces of a tooth after 48 hours in demineralization solution. The demineralized regions appear white and are contained in the 2x2 window.

C. Methods of Imaging

NIR- Transillumination

The NIR transillumination imaging set-up for buccal lesions is shown in Figure 4. Light from a single-mode fiber-pigtail coupled to a 1310-nm superluminescent diode (SLD) with an output power of 15-mW and a 30-nm bandwidth, Model SLED1300D20A (Optospeed, Zurich, Switzerland), was connected to a 20-mm NIR fibercollimator (Micro Laser Systems, Garden, Grove, CA). Crossed NIR polarizers, Model K46-252 (Edmund Scientific, Barrington, NJ), were used to remove light that directly illuminated the array without passing through the tooth.



Figure 4 NIR Transillumination setup for buccal lesions. The NIR light comes behind the tooth and travels through cross polarizers before reaching and illuminating the tooth. The InGaAs focal plane array is in front of the tooth and takes an image of the buccal surface of the tooth.

An InGaAs focal plane array (318x252 pixels), the Alpha NIR (Indigo Systems, Goleta, Ca) with an Infinimite lens (Infinity, Boulder, Co), was used to acquire all the images. The acquired 12 bit digital images were analyzed using IRVista software (Indigo systems, Goleta, CA). The illuminating light intensity, source to sample distance, and aperture diameter were adjusted for each sample to obtain the maximum contrast between the lesion and sound enamel without saturation of the InGaAs FPA around the lesion area. An example of an image produced by this method is shown in Figure 5.

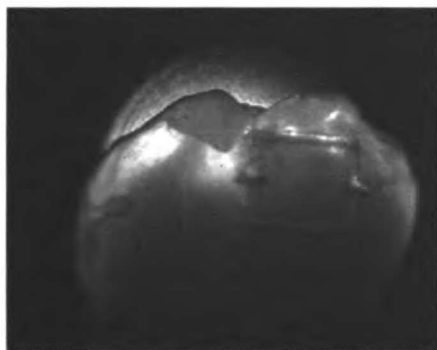


Figure 5. Buccal NIR transillumination image taken with the setup shown in figure 4. The transparency of the enamel in the NIR is apparent. The demineralized region within the 2x2 window appears darker than the surrounding enamel.

For occlusal images, the 20-mm collimated beam was focused by a 150-mm focal length cylindrical lens at a point just above the dentinal-enamel junction, as shown in Figure 6. This configuration was found to reflect a fairly uniform intensity level across the occlusal plane(Buhler, 2005)

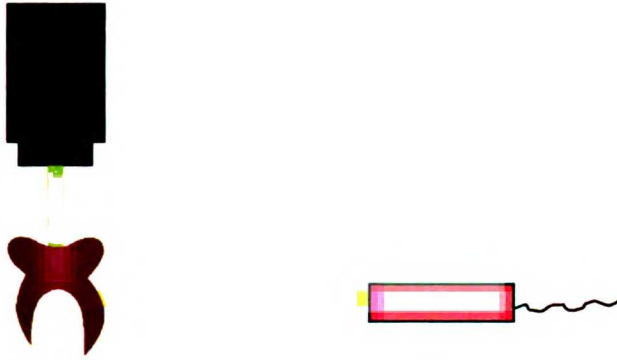


Figure 6 NIR Transillumination occlusal imaging setup. The NIR light comes from behind the tooth and enters the tooth just above the DEJ and is scattered by the dentin. The camera is positioned directly above the occlusal surface of the tooth.

The NIR light enters the teeth just above the DEJ and is scattered by the dentin. The light migrates towards the surface of the crown, into the occlusal surface of the tooth. An example of an image obtained with this method is shown in Figure 7.



Figure 7 Example of Transillumination-NIR occlusal image. The demineralized region appears darker than the surrounding sound enamel.

NIR- Reflectance Imaging with Polarization

NIR Reflectance Imaging with polarization images were taken with the same light sources, as shown in Figure 8. The NIR light was shined directly at the tooth, and

reflected light coming out of the tooth was imaged (Figure 8a). For occlusal images, the tooth was turned on its side so the light was incident on the occlusal surface (Figure 8b).

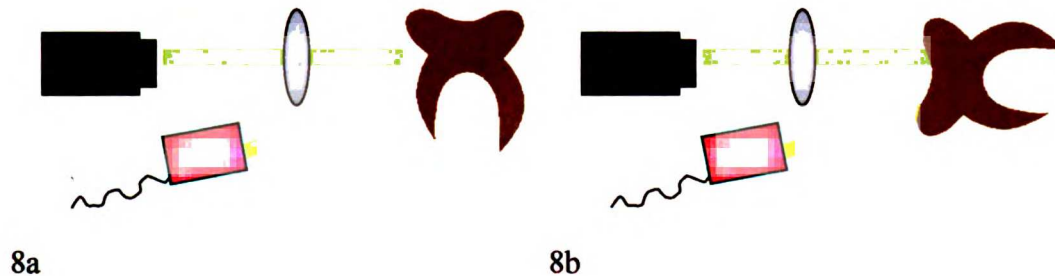


Figure 8 NIR reflectance imaging with cross polarization setup for buccal and occlusal lesions. 8A) The NIR light comes into the tooth at an angle, and the image is captured with the camera aimed at the buccal surface. 8B) The occlusal image is obtained with the same setup. The tooth is turned on its side so the occlusal surface is positioned in front of the camera.

The illuminating light intensity, source to sample distance, and aperture diameter were adjusted for each sample to obtain the maximum contrast between the lesion and sound enamel without saturation of the InGaAs FPA around the lesion area. An example of images obtained with NIR reflective with cross polarization is shown in Figure 9. In this method, the demineralized region appears lighter than the sound enamel. This is because the demineralized region scatters the light, and thus, more light is reflected back at the camera, causing the demineralized region to appear lighter.



Figure 9 Buccal and occlusal NIR reflective with polarization images. The demineralized region appears lighter than the surrounding sound enamel.

Near Infrared Single Fiber Probe

An image of the single fiber probe used is shown in Figure 10. A fiber probe was also used to “inject” near-IR light into the tooth at various angles on the occlusal surface to effectively “back-light” the surface lesions. The probe light was linearly polarized using an in-line polarizer and a polarizer was placed in front of the camera for cross-polarization images.

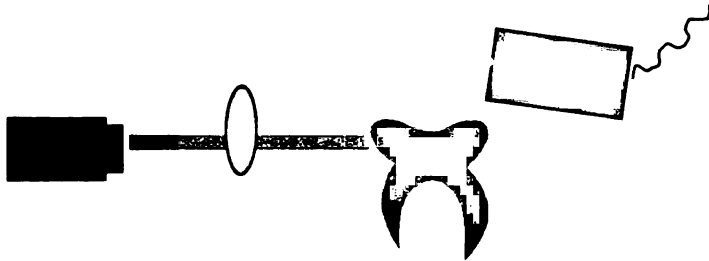


Figure 10 NIR Single Fiber Probe - NIR with polarization . The probe directs the NIR onto the occlusal surface of the tooth. Crossed polarizers were used to block out unwanted light. The image was taken from the buccal surface of the tooth.

The NIR light intensity, source to sample distance, and aperture diameter were adjusted for each sample to obtain the maximum contrast between the lesion and sound enamel without saturation of the InGaAs FPA around the lesion area. No occlusal images were taken with this method. Figure 11 shows an example of an image taken with the single fiber probe.

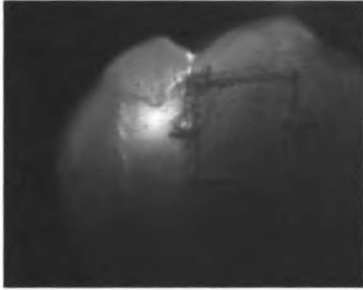


Figure 11 Buccal single fiber probe – NIR image. The demineralized region in the 2x2 window appears darker than the surrounding sound enamel.

Qualitative Light Fluorescence

Enamel surfaces were irradiated with a frequency doubled diode pumped solid state Nd:YVO₄ laser ($\lambda=473\text{-nm}$; DPSS Laser Model BLM-50; Extreme lasers, Houston Texas) with an incident intensity of up to 50-mW. A 500-nm long-pass filter (LP-500) and a DFK 31AF03 FireWire camera (resolution 1024 x 768) from the Imaging Source (Charlotte, NC) were used to image the fluorescence from the surface. Imaging was carried out in the dark to avoid the interference of ambient light. Figure 12 shows an example of images taken with QLF.

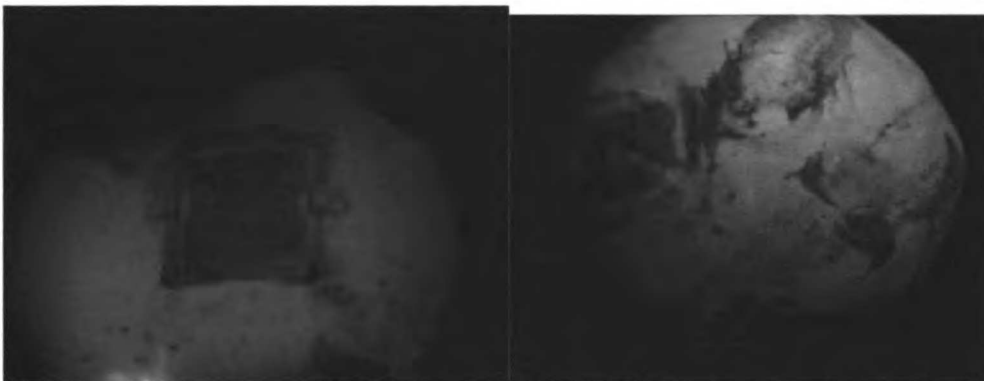


Figure 12 Buccal and Occlusal QLF image. The demineralized region appears darker than the surrounding sound enamel.

Visible Light Reflectance with Cross Polarization

For visible light reflectance with polarization, the same fiber-optic illuminator was used to illuminate the tooth. A color 1/3 firewire CCD camera with a resolution of 450 lines,

(Model DFK 5002/N, Imaging Source, Charlotte, NC), equipped with the same Infinimite lens, recorded the projection image. A buccal and occlusal image was obtained for each sample, as shown in Figure 13.

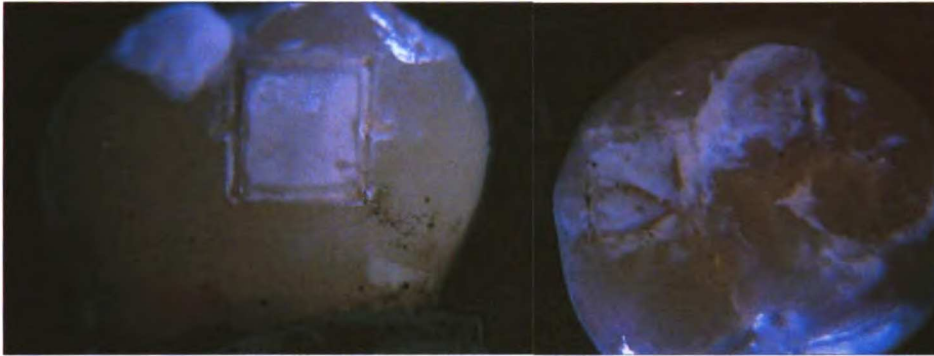


Figure 13 Buccal and occlusal visible with cross polarziation images. The demineralized region appears lighter than the surrounding sound enamel.

D. Methods of Image Analysis

All images were analyzed using the Igorpro software (Wavemetrics, Lake Oswego, OR).

A line profile was taken in the bottom $\frac{1}{2}$ of the window, as shown in Figure 14. Using the IgorPro software, a graph of the line out was generated, as shown in Figure 15.

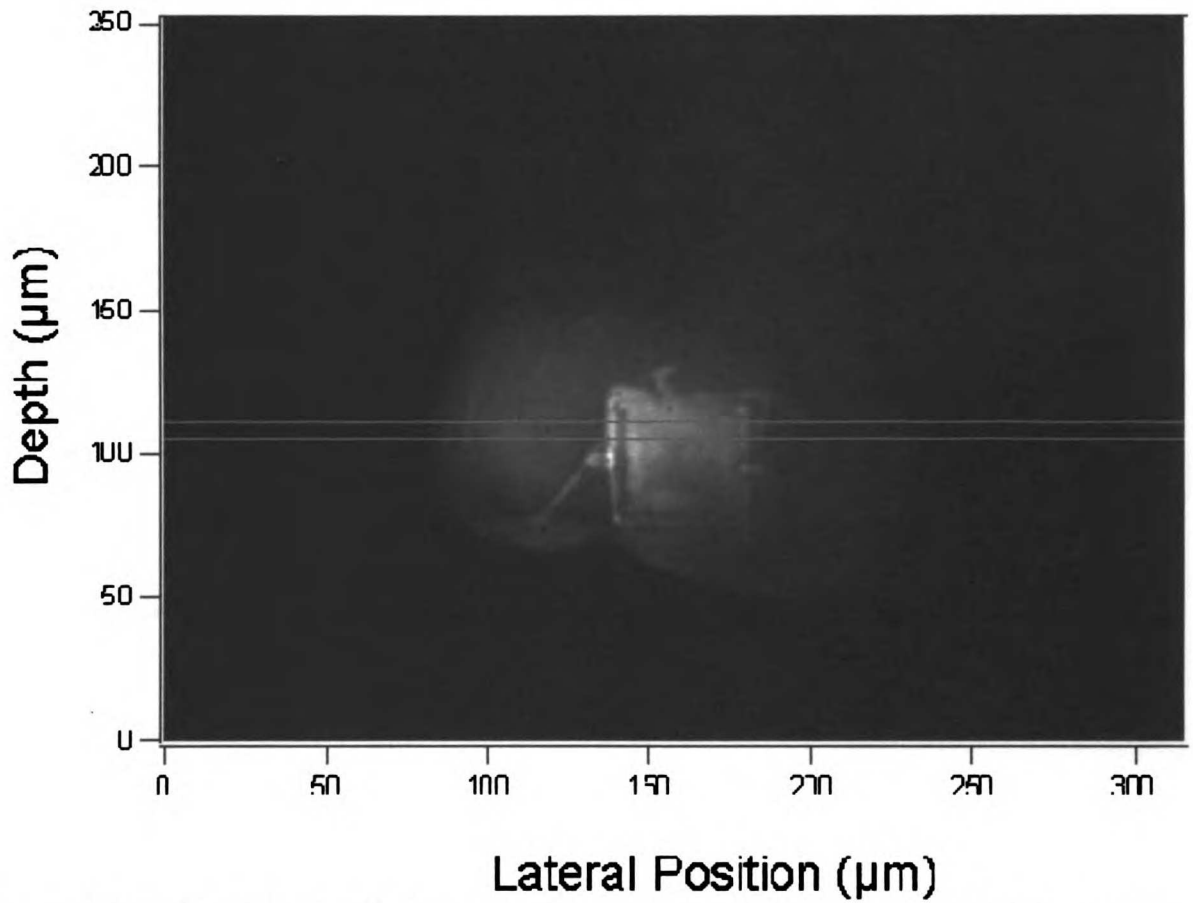


Figure 14 Example of a line profile taken through the image. The two blue lines show the boundaries of the position of the line profile, which is centered half way through the bottom half of the demineralized area.

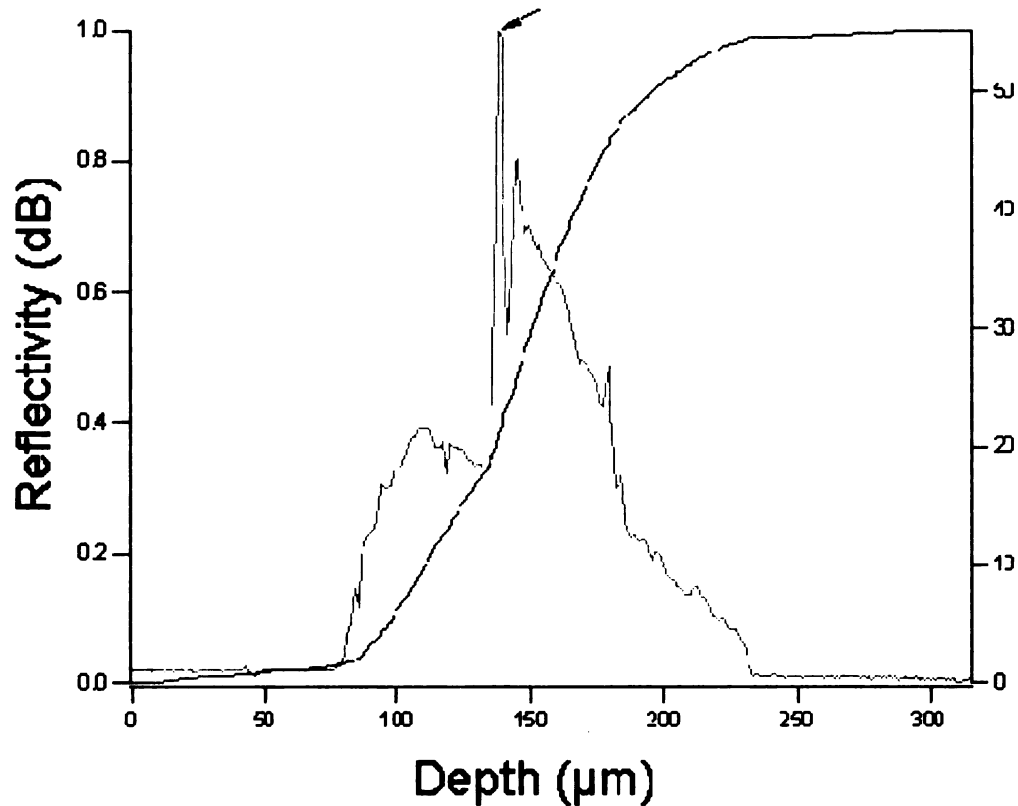


Figure 15. This graft is the line profile from the image in Figure 14. The x-axis represents the distance across the tooth. The Y-axis represents the reflectivity along the position. The red line represents the line profile, and the blue line represents the integration of the line profile.

The mean pixel intensity of the lesion and the sound enamel was measured using the IRvista software. Lesion contrast was calculated for each sample with the following equation:

$$\text{Lesion contrast (C)} = (I_S - I_L) / I_S$$

Where I_S is the mean intensity of the sound enamel, and I_L is the mean intensity of the lesion. Lesion contrast is defined as a ratio between 0 to 1. A greater number represents a higher contrast. $(I_L - I_S) / I_L$ was used for reflectance measurements that have reverse contrast, i.e., the intensity in lesion areas is higher than for the sound enamel

PS-OCT (Polarization Sensitive – Optical Coherence Tomography)

1. PS-OCT Imaging

An all single-mode fiber autocorrelator-based Optical Coherence Domain Reflectometry system(OCDR; Optiphase, Inc., Van Nuys, CA) was used for PS-OCT imaging and is well described in previous studies.(Bush, 2000; Fried, 2002) This system used a polarization switching probe, high efficiency piezoelectric fiber-stretchers and an InGaAs receiver.

The OCDR was integrated with a broadband high power superluminescent diode (SLD) (Denselight, Jessup, MD) with an output power of 45 mW and a bandwidth of 35-nm and a high-speed XY-scanning system (ESP 300 controller & 850HS stages, National Instruments, Austin, TX) for *in vitro* optical tomography. The probe was designed to provide a spot diameter of 50 μm over a range of 10 mm.

Six hundred scans were taken in the x-axis at 20 μm intervals, and 3 scans in the y-axis at a distance of 200 μm . The scans were taken across the lower half of the 2x2 window, where the area of interest lies.

3. PS-OCT Line Profiles

In a perpendicular-axis PS-OCT image, the demineralized regions can be analyzed due to the higher reflectivity. In each sample, two line profiles were taken: one in the demineralized region, and one in the sound region. The position of the line profile was taken at the center of the lesion, or the center of the sound enamel (Figure 16).

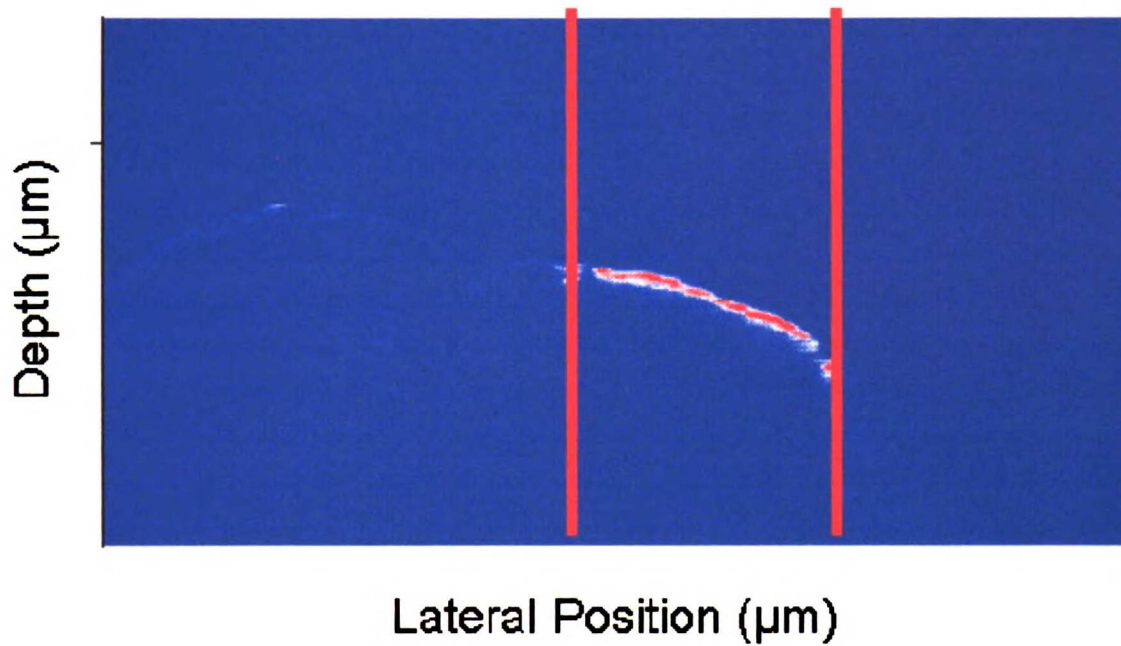


Figure 16 Image of a line profile taken through the center of the demineralized region. The y-axis represents the axial distance into the tooth. The x-axis represents the distance along the tooth surface. The lesion area is shown between the two red lines.

To assess the lesion severity, the integrated reflectivity, ΔR (dB x μm) was measured along the integration line from the surface of the enamel to a point 400 μm into the tooth along the axial depth, or x-axis. The difference in the y-axis between the two points represents the ΔR (Figure 17).

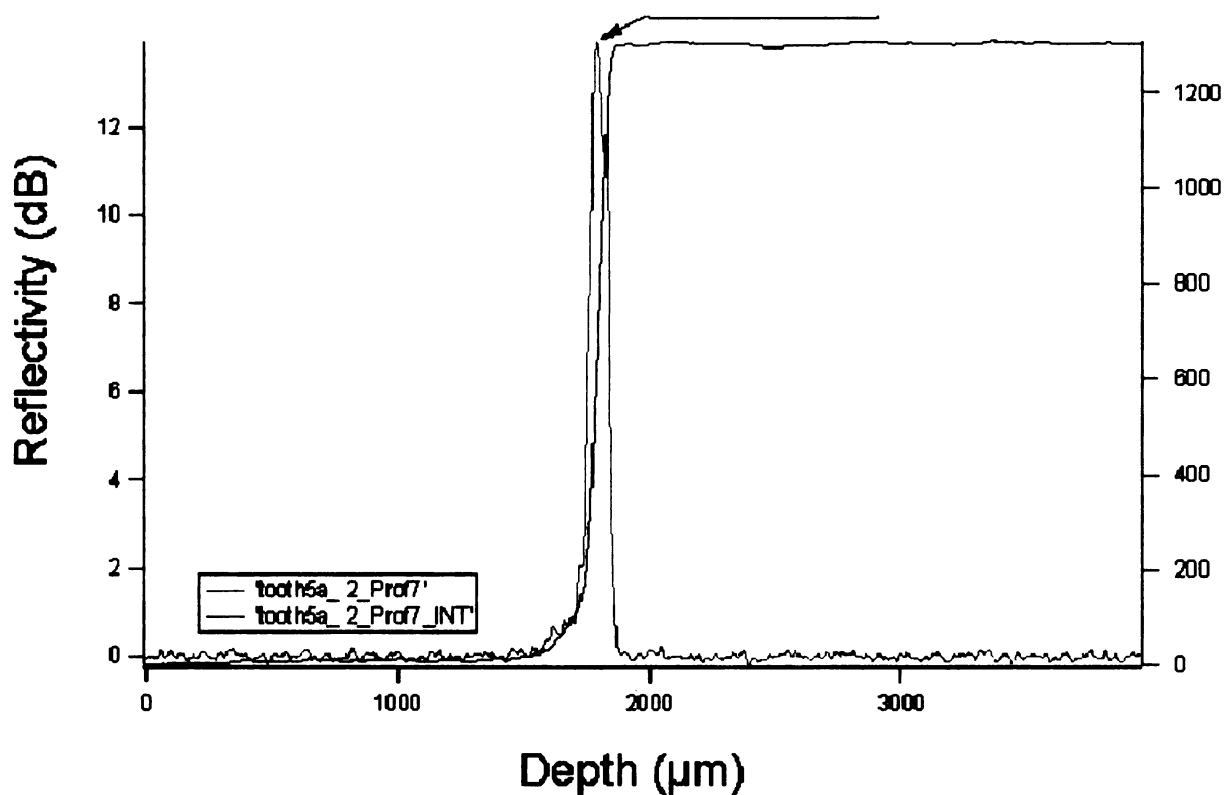


Figure 17 Integrated line profile with markers at the surface and a point 400 μm into the tooth, along the x-axis in an area with a lesion. The red line represents the line profile. The blue line is the integration of the line profile. The background reflectivity is zeroed.

Results

A. Buccal Images

Image contrast values were obtained for all buccal lesions using the IgorPro software. The following table, Table 1, shows all the image contrast values for the 15 buccal lesions using the five different imaging methods. A greater number represents a larger contrast. A negative number occurs when a demineralized region appears lighter than the sound region when it should appear darker.

Table 1 Buccal image contrast values of the five different imaging methods for all 15 teeth. A higher number depicts a larger contrast. A negative number occurs when the lesion appears lighter when it should appear darker than the sound enamel.

	Visual Reflectance with cross polarization	NIR Reflectance with cross polarization	NIR Transillumination with cross polarization	NIR Single Fiber Probe with cross polarization	QLF
1	0.2295	0.2295	0.2441	0.5536	0.9187
2	0.3016	0.4077	-0.0172	0.4958	0.2830
3	0.2387	0.8474	0.1297	0.4508	0.5667
4	0.3038	0.8263	0.3834	0.5349	0.1819
5	0.4419	0.6615	0.2953	0.5815	0.1838
6	0.0539	0.6688	0.2578	0.5425	0.6476
7	0.3866	0.7887	0.4175	0.4764	0.6134
8	0.2571	0.6681	0.2442	0.4278	0.0086
9	0.2704	0.7253	-0.0862	0.2447	0.4469
10	0.2341	0.6091	-0.2275	0.4161	0.4796
11	0.0343	0.6497	0.2719	0.1682	0.0238
12	0.2294	0.7420	0.3272	0.0126	0.5995
13	0.1035	0.3470	0.0133	-0.6040	0.6337
14	0.3279	0.6046	0.2704	-0.1728	0.5532
15	0.1181	0.6315	0.2103	0.3706	0.4849

Table 2 and Figure 13 show the mean image contrast values for each method, and the standard deviations for each method. NIR Reflectance with cross polarization has

the highest mean image contrast value, while NIR Transillumination has the lowest image contrast value.

Table 2 Buccal image contrast means and standard deviation for the 5 different imaging methods

Groups	Mean	SD
Visible Reflectance with cross polarization	0.2354	0.1163
NIR Reflectance with cross polarization	0.6271	0.1748
NIR Transillumination with cross polarization	0.1823	0.1833
NIR Single Fiber Probe with cross polarization	0.2999	0.3304
QLF	0.4417	0.2555

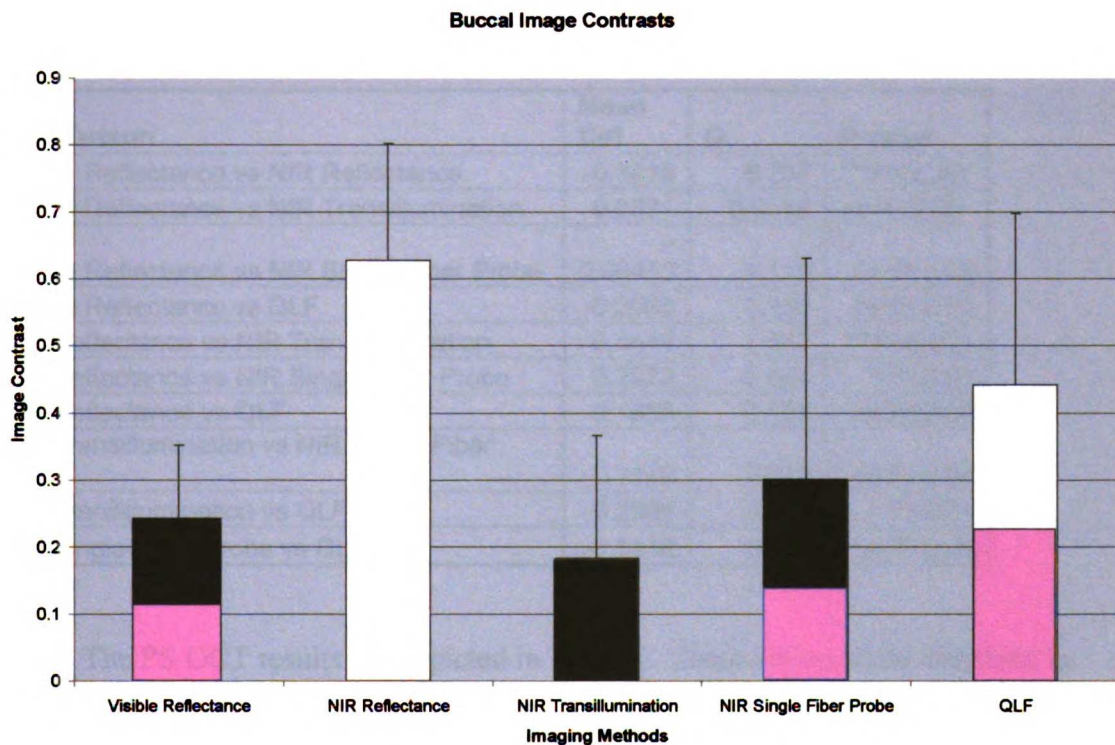


Figure 18 Buccal image contrast means with standard deviation. The error bars represent standard deviations. Bars with the same color are not significantly different from each other, $P > 0.05$.

A one-way analysis of variance (ANOVA) followed by the Tukey-Kramer post-hoc multiple comparison test was used. The results, with the P-values are shown in Table

3. The NIR reflectance imaging with cross polarization group had the highest mean

image contrast, and was significantly greater than the conventional visual reflectance with cross polarization, NIR single fiber probe with cross polarization, and NIR transillumination with cross polarization groups. The NIR transillumination with cross polarization group showed the lowest image contrast. There was no statistically significant difference between QLF and NIR single fiber probe, and no significant difference between the NIR transillumination with cross polarization group and the NIR single fiber probe group. The visual reflectance group was only statistically significantly different from the NIR reflectance group.

Table 3 Results of ANOVA followed by the Tukey-Kramer post-hoc multiple comparison test.

Comparison	Mean Diff	Q	P value
Visible Reflectance vs NIR Reflectance	-0.3918	6.757	***P<0.001
Visible Reflectance vs NIR Transillumination	0.0531	0.9158	ns P>0.05
Visible Reflectance vs NIR Single Fiber Probe	0.06453	1.113	ns P>0.05
Visible Reflectance vs QLF	-0.2063	3.558	ns P>0.05
NIR Reflectance vs NIR Transillumination	0.4449	7.672	***P<0.001
NIR Reflectance vs NIR Single Fiber Probe	0.3272	5.644	**P<0.01
NIR Reflectance vs QLF	0.1855	3.199	ns P>0.05
NIR Transillumination vs NIR Single Fiber Probe	-0.1176	2.029	ns P>0.05
NIR Transillumination vs QLF	-0.2594	4.474	* P<0.05
NIR Single Fiber Probe vs QLF	-0.1418	2.445	ns P>0.05

The PS-OCT results are depicted in Table 4. These values show that there is significant demineralization in all the buccal lesions. A higher value of the integrated reflectivity in the lesion areas shows that there is greater demineralization. The mean integrated reflectivity in units of ΔR (dB x μm) to a depth of 200- μm were 1896+/- 655 for the lesion and 196 +/- 141 for the sound area. Based on previous comparisons of ΔR vs ΔZ , the ΔR should translate to integrated mineral loss (ΔZ) values of approximately 2000 (vol% x μm)

Table 4 Buccal OCT values for all 15 teeth. A high number in the lesion and a low number in the sound shows that there is demineralization in areas of interest.

Tooth	Buccal OCT	
	Lesion	Sound
1	1704.21	105.102
2	1687.26	179.16
3	1845.92	108.518
4	546.313	192.123
5	1453.12	106.356
6	1127.18	179.457
7	2387.04	140.424
8	1648.14	378.013
9	1233.94	134.94
10	1473.36	250.226
11	1853.65	92.4433
12	2290.43	190.706
13	1927.64	204.781
14	2021.93	142.281
15	1128.82	283.134

B. Occlusal Images

The results of the image contrast analysis for the occlusal lesions on the 15 teeth are reported in Table 5. Higher image contrast values reflect a greater contrast between demineralized and sound enamel.

Table 5 Image contrast values for the 5 different occlusal methods. A higher number represents a greater contrast between sound and demineralized enamel.

	Visible Reflectance	NIR Reflectance	QLF	NIR Transillumination
1	0.2764	0.5914	0.6202	0.6764
2	0.2795	0.2430	0.3663	-0.1380
3	0.4139	0.7556	0.7306	0.1369
4	0.0622	0.7436	0.5021	-0.1847
5	0.2635	0.5834	0.4101	-0.3537
6	0.3979	0.6669	0.4947	0.4374
7	0.2036	0.5968	0.4420	0.2508
8	0.4816	0.3502	0.1528	0.5666
9	0.4476	0.6835	0.4472	0.5294
10	0.4433	0.7423	0.4446	-0.5497
11	0.0887	0.7976	0.7632	0.3515
12	0.2416	0.6032	-0.1564	-0.0478
13	0.3536	0.8189	0.2815	-0.6627
14	0.0090	0.4541	0.1959	-0.3819
15	0.2963	0.8696	0.9105	-0.5464

Table 6 and Figure 14 show the average image contrast for each method, and the standard deviations with each method. The one-way analysis of variance (ANOVA) followed by the Tukey-Kramer post-hoc multiple comparison test was also used. The results, with the P-values are shown in Table 7. The NIR reflectance group had the highest mean image contrast that was significantly greater than the visual reflectance and NIR transillumination groups. The NIR transillumination group showed the lowest image contrast and the greatest standard deviation. There was no significant difference between NIR reflectance and QLF groups, and no significant difference between visual reflectance

and QLF groups. Figure 14 is a chart that shows the differences and similarities between groups.

Table 6 The mean and standard deviations for the 4 different occlusal imaging methods.

Group	Mean	SD
Visible Reflectance	0.2839	0.1458
NIR Reflectance	0.6333	0.1755
NIR Transillumination	0.005614	0.4489
QLF	0.4403	0.2644

Table 7 ANOVA followed by Tukey Kramer post-hoc results with P values

Comparison	Mean Diff	Q	P value
Visible Reflectance vs NIR Reflectance	0.3494	4.759	** P < 0.01
Visible Reflectance vs QLF	0.1564	2.13	ns P>0.05
Visible Reflectance vs NIR Transillumination	0.2783	3.79	* P<0.05
NIR Reflectance vs NIR Transillumination	0.6277	8.549	*** P<0.001
NIR Reflectance vs QLF	0.193	2.629	ns P>0.05
NIR Transillumination vs QLF	0.4347	5.921	*** P<0.001

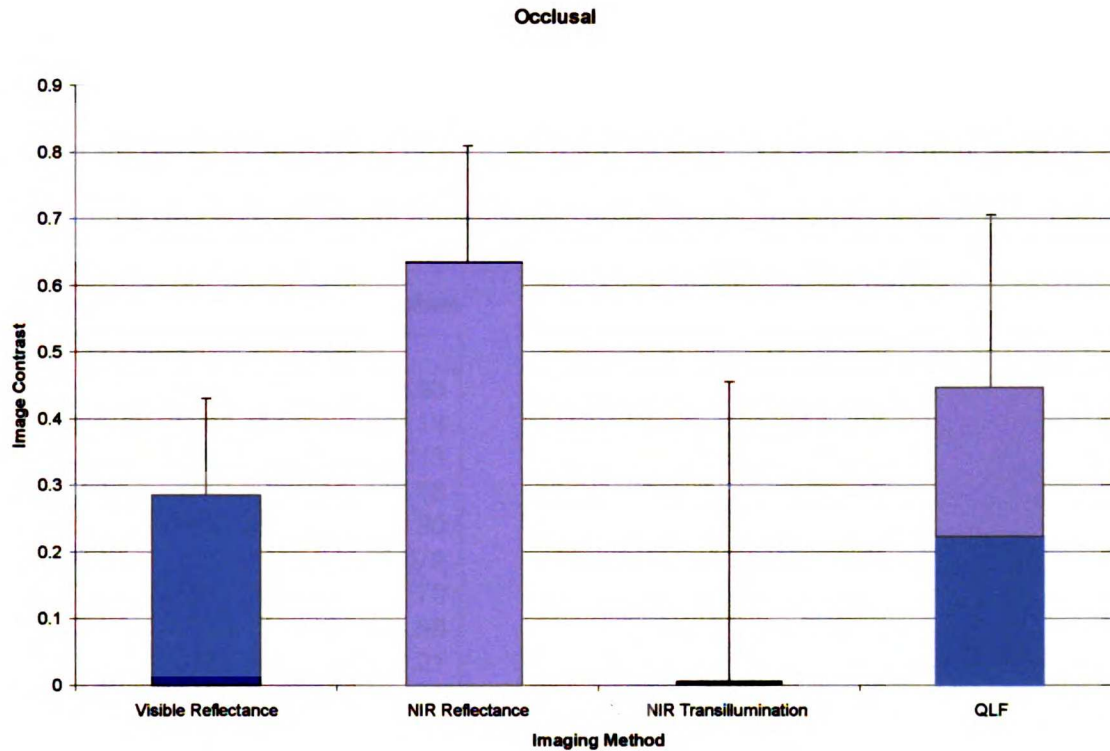


Figure 19 Occlusal image contrast means with standard deviation. The error bars represent standard deviations. Bars with the same color are not significantly different from each other, $P>0.05$.

The NIR reflectance imaging group had the highest mean, with a value of .0633. This was statistically significant from the visible reflectance group, but not with the QLF group. QLF, however is not shown to be statistically significant from the visible reflectance group. NIR transillumination had the lowest image contrast numbers, with a large standard deviation.

PS-OCT values reflect the severity of the lesions. These numbers are shown in Table 8. These numbers show that there is demineralization in the lesions. The mean integrated reflectivity in units of ΔR (dB x μm) to a depth of 200- μm were 1622 +/- 482 for the lesion and 179 +/- 78 for the sound area.

Table 8 Occlusal OCT Reflectivity Values

Tooth	Lesion	Sound
1	2979.55	252.93
2	2047.75	242.14
3	1445.61	161.13
4	2895.03	116.16
5	1638.35	150.30
6	641.28	60.075
7	1311.15	171.70
8	2105.15	121.88
9	1562.09	82.31
10	1169.81	277.36
11	2494.58	112.89
12	1846.44	186.47
13	1594.66	151.66
14	2188.94	196.35
15	2526.97	656.03

Discussion

The purpose of this study was to test the hypothesis that we can measure significant differences in optical contrast at 1310 nm between sound and artificially demineralized enamel on the buccal and occlusal surfaces, and to test the hypothesis that NIR imaging manifests greater contrast than other promising methods, including qualitative light fluorescence and visible reflectance with cross-polarization.

NIR reflectance images with cross polarization provided the highest contrast, and can most effectively detect early demineralization on both smooth surfaces and occlusal surfaces. This was the only method that provided significantly higher contrast than visible reflectance images with cross-polarization. NIR reflectance images of both buccal and occlusal surface demineralization show high image contrast and demonstrate that NIR imaging can be used for detection and quantification of early surface white spot lesions. This novel method exploits the high transparency of dental enamel at 1310 nm. We have shown that by imaging teeth with early surface demineralization, that NIR technology can be superior in performance to visual and similar to QLF methods.

The NIR transillumination method did not show high image contrast between sound and demineralized areas. In buccal images, it was difficult to find contrast between the sound and demineralized regions. In the NIR transillumination method, the near infrared light comes from behind the tooth and has to travel through the entire tooth, including the dentin. The dentin may have scattered the light in such a way that there was not enough light to pass through the entire tooth or take an indirect path through the highly transparent enamel in order to reach the lesion areas. In the latter case, the light may strike the lesion at large angles, causing an increase in the emitted light as opposed

to a decrease. While the demineralized regions should appear darker, there were samples where the demineralized regions actually appeared lighter. In areas where there was no dentin to scatter the light, the sound enamel appeared translucent, and a greater contrast was achieved. However, in areas where the lesion was lower on the tooth, where there was dentin behind the lesion, it was difficult to see the lesion due to the intervening dentin that scattered the light, as can be seen in Tooth 5 in the appendix. It appears that the transillumination method has difficulties for very shallow lesions using this imaging geometry, and is better for deeper and more severe lesions. Another study is needed that examines the contrast levels as the demineralization increases to see how the contrast increases using the transillumination method. It is also possible that the angle in which the light hits the tooth makes a difference, since there are some teeth that show a greater contrast using the transillumination method than others. Future studies will investigate whether the imaging geometry explains these differences.

We found that with the NIR single fiber probe, the direction in which the probe is aimed at the tooth changes the image greatly. Thus, it is possible that we did not find the greatest contrast in our images because we did not take different images with different positions of the probe. However, the contrast that we found was still greater than the visible reflectance imaging. Similar to the NIR transillumination imaging, the light has to travel through the highly scattering dentin, resulting in lower contrast values.

Our study is in agreement with previous studies that found that QLF has greater sensitivity for early caries lesions on smooth surfaces. We were able to obtain high image contrast for QLF on both the buccal and occlusal lesions. In previous work that compares QLF with visible reflectance imaging, the visible reflectance imaging did not

employ cross polarization to enhance the image contrast of the reflectance measurements. Studies have not yet shown that QLF is effective on occlusal lesions, however, it performed well in our studies. We were able to provide a high contrast on occlusal images. While QLF has shown to be a promising method in imaging demineralization, one disadvantage is the influence of ambient light. Therefore, the imaging needs to be done in the dark or other means are needed to reduce the ambient light. This problem can be overcome by electronically gating the light using a modulated light-source for excitation and a lock-in amplifier for detection. Furthermore, QLF is designed for very early lesions in which the demineralization is localized and is not good at detecting subsurface lesions. Also, a typical orthodontic lesion usually spreads widely around the bracket. Imaging with QLF would be difficult because it would be difficult to capture a QLF image with optimal light intensity in any part of the lesion.(Aljehani et al., 2004)

This study is the first attempt at using clear varnish to prevent demineralized regions. Previous studies have used red varnish, and the red varnish was removed prior to imaging. While the clear varnish is effective at providing a barrier and preventing demineralized regions while not interfering with imaging, it was also difficult to tell visually whether or not the varnish uniformly covered the surface. There were areas where the clear varnish had peeled off, or chipped off, making the demineralized regions more difficult to identify. Also, in many of the samples, the lesion was not uniform in the 2x2 square, due to the fact that the varnish was not applied correctly. In the future, two coats of varnish should be applied to ensure that every surface is definitely completely covered with clear varnish. The teeth should be handled with care to prevent any varnish

from chipping off the tooth. Also, for occlusal surfaces, attempts should be made to ensure that the varnish does not flow into the grooves on the occlusal surface.

Initially, we measured the contrast by averaging the sound enamel contrast levels from both the right and left sides. This became a problem in some of the samples where the illuminating light was not uniform; the sound enamel appeared darker on the side opposite to where the light was coming in from. In these cases, sound enamel appeared darker, not because there was demineralization, but because there was no light in that area. Therefore, we decided to choose the side of sound enamel that appeared the brightest, so we could determine the highest contrast between sound and demineralized enamel.

In determining the line profile taken for the demineralized enamel, we took an area in the middle of the bottom half of the demineralized region. An attempt was made to take the line profile on the same area of each tooth with the different methods. Taking a second line profile in approximately the same area could result in a slightly different image contrast value. Future studies should take multiple line profiles on the same tooth to determine any variation in image contrasts that would result in a line profile taken at a slightly different position, and the results should be averaged to account for any possible variation.

Another problem we encountered was the dark bacterial spots which appeared on the samples over time, despite the fact that the samples were stored in thymol. This made imaging difficult in later images because both the bacterial spots and the demineralized regions appeared darker in the images. When analyzing the images, care was taken to

ensure that demineralized regions that we measured did not contain any bacterial spots. In future studies, more effort should be made to keep the teeth clean and bacteria-free.

Early studies have shown that fluorosis, pigmentation, and staining do not significantly interfere with imaging demineralization in the NIR. Thus, imaging in the NIR is more effective in determining demineralized lesions because it eliminates confounding variables that interfere significantly with visual diagnosis of dental decay and cause false positives in fluorescent caries detection methods.(Christopher M. Buhler, 2005) Although the results do not show a statistically significant difference between NIR and QLF, this is a valuable advantage that NIR has over QLF. QLF does not distinguish between staining and demineralization, whereas NIR does. Imaging in the NIR with cross-polarization provides excellent contrast because light scattering in the sound enamel is weak, and it is increased in demineralized regions. This method provides superior contrast over visible reflectance imaging with cross polarization because scattering in sound enamel is high in the visible.

The principal drawback of NIR at the present time is the high cost of the InGaAs technology. Near infrared imaging is more cost effective at shorter wavelengths. At 830 nm, the technology is more affordable, however the performance has not been evaluated. Future studies could examine the imaging contrast at shorter wavelengths to determine if the contrast is sufficiently higher than in the visible. It is likely that lower cost NIR technology will become available in the future.

Previous studies have shown that PS-OCT correlates with the gold standard of microradiography and with the polarized light microscopy. Thus, we used PS-OCT to

determine the depth of the exposed demineralized lesion. The results show that the lesions were all present in the areas with significant demineralization.

PS-OCT can be used in tandem with NIR imaging to acquire specific depth resolved images of the lesion depth and severity in suspect areas defined in the NIR image and both of these NIR imaging systems can share similar broadband light sources. Future studies will investigate the ability of the NIR to detect the repair of early surface demineralization.

Further research is required to ensure that these results can be repeated *in vivo*. NIR imaging is a potentially useful tool to the orthodontic community. Quantification of lesion severity is better, compared to the qualitative and subjective analysis obtained by visual examination. Future work is needed to determine if NIR can evaluate changes in depth of the demineralization

Conclusion

This study clearly demonstrates that a NIR imaging system has considerable potential for imaging of early surface demineralization of sound enamel. The highly promising images of demineralized lesions suggest that NIR reflectance imaging with cross-polarization can be a useful tool for routine monitoring of white spot lesions during orthodontic treatment. Another advantage of this method is that it enables the dentist to treat early dental decay effectively in a non-surgical manner, as these lesions can be treated with fluoride therapy. Because NIR wavelengths are safe, the dentist can acquire multiple NIR images of the lesions during subsequent visits to determine if fluoride therapy is effective in arresting the lesion or whether the lesion has expanded, requiring

more aggressive intervention. Such an approach is not practical with radiographic methods due to repeated x-ray exposure. In addition to the high contrast in this study, another advantage NIR imaging has over QLF is the potential ability to distinguish caries from stains and fluorosis. Since NIR wavelengths are safe, there are no health risks. Thus, NIR imaging can be a system that allows the clinician to acquire a series of images to better understand the progression of the lesion.

References

A. Baumgartner SD, C.K. Hitzenberger, H. Sattmann, B. Robi, A. Moritz, W. Sperr, and A.F. Fercher (2000). Polarization-sensitive optical coherence tomography of dental structures. *Caries Res* 34(59-69.

Al-Khateeb S, Forsberg CM, de Josselin de Jong E, Angmar-Mansson B (1998). A longitudinal laser fluorescence study of white spot lesions in orthodontic patients. *Am J Orthod Dentofacial Orthop* 113(6):595-602.

Aljehani A, Tranaeus S, Forsberg CM, Angmar-Mansson B, Shi XQ (2004). In vitro quantification of white spot enamel lesions adjacent to fixed orthodontic appliances using quantitative light-induced fluorescence and DIAGNOdent. *Acta Odontol Scand* 62(6):313-8.

Amaechi BT, Higham SM (2002). Quantitative light-induced fluorescence: a potential tool for general dental assessment. *J Biomed Opt* 7(1):7-13.

Ando M, Hall AF, Eckert GJ, Schemehorn BR, Analoui M, Stookey GK (1997). Relative ability of laser fluorescence techniques to quantitate early mineral loss in vitro. *Caries Res* 31(2):125-31.

Ando M, Schemehorn BR, Eckert GJ, Zero DT, Stookey GK (2003). Influence of enamel thickness on quantification of mineral loss in enamel using laser-induced fluorescence. *Caries Res* 37(1):24-8.

Ando M, Eckert GJ, Stookey GK, Zero DT (2004). Effect of imaging geometry on evaluating natural white-spot lesions using quantitative light-induced fluorescence. *Caries Res* 38(1):39-44.

Angmar-Mansson B, ten Bosch JJ (1987). Optical methods for the detection and quantification of caries. *Adv Dent Res* 1(1):14-20.

Benson P SA, Willmot D (2007). Polarized Versus Nonpolarized Digital Images for the Measurement of Demineralization Surrounding Orthodontic Brackets. *Angle Orthod* 78(2):288-293.

Benson PE, Pender N, Higham SM (2003). Quantifying enamel demineralization from teeth with orthodontic brackets—a comparison of two methods. Part 1: repeatability and agreement. *Eur J Orthod* 25(2):149-58.

Benson PE, Shah AA, Millett DT, Dyer F, Parkin N, Vine RS (2005a). Fluorides, orthodontics and demineralization: a systematic review. *J Orthod* 32(2):102-14.

Benson PE, Shah AA, Willmot DR (2005b). Measurement of white lesions surrounding orthodontic brackets: captured slides vs digital camera images. *Angle Orthod* 75(2):226-30.

Boersma JG, van der Veen MH, Lagerweij MD, Bokhout B, Prahl-Andersen (2005). Caries prevalence measured with QLF after treatment with fixed orthodontic appliances: Influencing factors. *Caries Res* 39(41-47).

Bosch JJt (1999). Summary of Research of Quantitative Light Fluorescence. Early Detection of Dental Caries II: Proceedings of 4th Annual Indiana Conference, Indianapolis, IN.

Bush J DP, Marcus M. (2000). All-fiber optic coherence domain interferometric techniques. *SPIE*:71-80.

Christopher M. Buhler PNaDF (2005). Imaging of occlusal dental caries (decay) with near-IR light at 1310-nm. *Optical Express* 13(2):573-582.

D. Fried JDBF, R. E. Glens, and W. Seka (1995). The nature of light scattering in dental enamel and dentin at visible and near-IR wavelengths. *Appl. Opt.* 34(1278-1285).

D. Fried JX, S. Shafi, J.D.B. Featherstone, T. Breunig, and C.Q. Lee (2002). Early detection of dental caries and lesion progression with polarization sensitive optical coherence tomography. *J Biomed Opt* 7(618-627).

Darling CL, Huynh GD, Fried D (2006). Light scattering properties of natural and artificially demineralized dental enamel at 1310 nm. *J Biomed Opt* 11(3):34023.

Eggertsson H, Analoui M, van der Veen M, Gonzalez-Cabezas C, Eckert G, Stookey G (1999). Detection of early interproximal caries in vitro using laser fluorescence, dye-enhanced laser fluorescence and direct visual examination. *Caries Res* 33(3):227-33.

Featherstone JD, Holmen L, Thylstrup A, Fredebo L, Shariati M (1985). Chemical and histological changes during development of artificial caries. *Caries Res* 19(1):1-10.

Featherstone JDaDY (1999). The need for new caries detection methods. *Lasers in Dentistry V, San Jose, CA Proc. SPIE* 3593(134-140).

Feldchtein FI GG, Gelikonov VM, Iksanov RR, Kuranov RV, Sergeev AM, Gladkova ND, Ourutina MN, Warren JA, Reitze DH (1998). In vivo OCT imaging of hard and soft tissue in the oral cavity. *Optical Express* 3(3):239-251.

Fried D, Featherstone JD, Darling CL, Jones RS, Ngaotheppitak P, Buhler CM (2005). Early caries imaging and monitoring with near-infrared light. *Dent Clin North Am* 49(4):771-93, vi.

Fried RJaD (2002a). Attenuation of 1310 and 1550-nm laser light through dental enamel. *Lasers in Dentistry VIII Proc. SPIE* 4610,(187-190

Fried RJaD (2002b). Attenuation of 1310 and 1550-nm laser light through dental enamel. *Lasers in Dentistry VIII, San Jose, Proc. SPIE* 5610(187-190.

Gorelick L, Geiger AM, Gwinnett AJ (1982). Incidence of white spot formation after bonding and banding. *Am J Orthod* 81(2):93-8.

Hafstrom-Bjorkman U, Sundstrom F, de Josselin de Jong E, Oliveby A, Angmar-Mansson B (1992). Comparison of laser fluorescence and longitudinal microradiography for quantitative assessment of in vitro enamel caries. *Caries Res* 26(4):241-7.

Jones RS (2006). Near Infrared Optical Imaging of Early Dental Caries. San Francisco, University of California, San Francisco.

Kanthathas K, Willmot DR, Benson PE (2005). Differentiation of developmental and post-orthodontic white lesions using image analysis. *Eur J Orthod* 27(2):167-72.

Lagerweij M, van der Veen M, Ando M, Lukantsova L, Stookey G (1999). The validity and repeatability of three light-induced fluorescence systems: An in vitro study. *Caries Res* 33(3):220-6.

Mattousch TJ, van der Veen MH, Zentner A (2007). Caries lesions after orthodontic treatment followed by quantitative light-induced fluorescence: a 2-year follow-up. *Eur J Orthod* 29(3):294-8.

Meller C, Heyduck C, Tranaeus S, Splieth C (2006). A new in vivo method for measuring caries activity using quantitative light-induced fluorescence. *Caries Res* 40(2):90-6.

Mitchell L (1992). Decalcification during orthodontic treatment with fixed appliances—an overview. *Br J Orthod* 19(3):199-205.

Ogaard B, Rolla G, Arends J (1988). Orthodontic appliances and enamel demineralization. Part 1. Lesion development. *Am J Orthod Dentofacial Orthop* 94(1):68-73.

Ogaard B (1989). Prevalence of white spot lesions in 19-year-olds: a study on untreated and orthodontically treated persons 5 years after treatment. *Am J Orthod Dentofacial Orthop* 96(5):423-7.

Pretty IA, Pender N, Edgar WM, Higham SM (2003). The in vitro detection of early enamel de- and re-mineralization adjacent to bonded orthodontic cleats using quantitative light-induced fluorescence. *Eur J Orthod* 25(3):217-23.

Robert S. Jones GDH, Graham C. Jones, Daniel Fried (2003). Near-infrared transillumination at 1310-nm for the imaging of early dental decay. *Optical Express* 11(18):2259-2265.

Spitzer D, Bosch JT (1975). The absorption and scattering of light in bovine and human dental enamel. *Calcif Tissue Res* 17(2):129-37.

Travess H, Roberts-Harry D, Sandy J (2004). Orthodontics. Part 6: Risks in orthodontic treatment. *Br Dent J* 196(2):71-7.

Wang XJ MT, deBoer JF, Zhang Y, Pashley DH, Nelson JS (1999). Characterization of dentin and enamel by use of optical coherence tomography. *Appl. Opt.* 38(10):2092-2096.

Willmot DR, Benson PE, Pender N, Brook AH (2000). Reproducibility of quantitative measurement of white enamel demineralisation by image analysis. *Caries Res* 34(2):175-81.

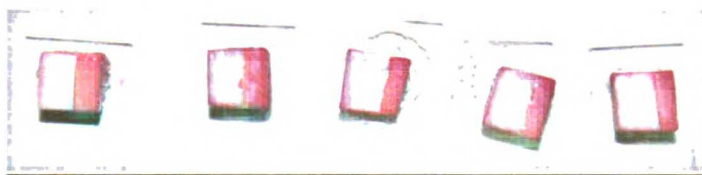
APPENDICES

Appendix A: Pilot Study

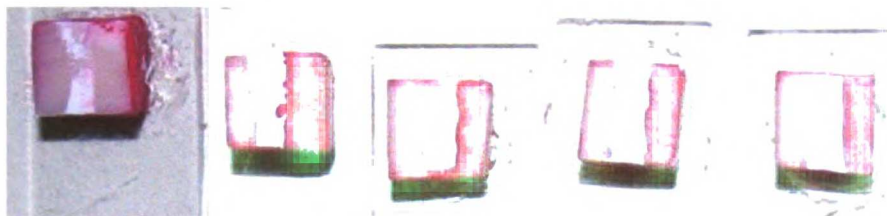
The purpose of the pilot study was to identify an optical adhesive that can serve as a reference background that does not change the optical properties of the tooth surface and is not changed optically by demineralization.

MATERIALS AND METHODS:

We tested with two translucent materials. An Optical adhesive (OA) designed for fiberoptics (Optical adhesive 81), which is UV cured, and an acid-resistant clear varnish (CV) (Clear, Revlon, New York). Five 5x5x2 mm sections of polished bovine enamel blocks were used in each group. An area of transparent material and an area of red varnish was painted on the bovine enamel blocks, with an area exposed so that the enamel would be subject to demineralization, as seen in the images below. The teeth were then placed for 5 days in a demineralization solution at pH 4.5. NIR and PS-OCT were used to determine if the transparent material prevented demineralization. The red varnish was removed prior to scanning with the NIR and PS-OCT, while the translucent material remained on the teeth.



Images of samples with clear varnish, pre-demineralization



Images of samples with clear varnish, post demineralization



Images of samples with optical adhesive, pre-demineralization



Images of samples with optical adhesive, post-demineralization

RESULTS:

Image Contrast

	OA	OA sound vs demin	CV	CV sound vs Demin
1	0.23	.200	0.200	0.189
2	0.135	.056	0.148	0.135
3	0.206	.101	0.242	0.049
4	0.195	.173	0.175	0.126
5	0.08	.057	0.135	0.683

These results for the Optical Adhesive sample show that the image contrast between sound and demineralized regions is similar to the image contrast between the optical adhesive and demineralized regions. Therefore, the optical adhesive does not change the optical properties.

With samples for the clear varnish, image contrast between clear varnish and demineralized regions were very similar to the image contrast between sound and demineralized regions. Therefore, the clear varnish does not change the optical properties of the tooth.

OCT Images – Integrated Reflectivity

	Nail Polish	Sound	Demin
dn1	68.1902	75.375	328.551
dn2	241.972	143.035	448.571
dn3	60.0098	97.7037	235.938
dn4	178.176	178.727	377.274
dn5	245.262	132.561	380.585
do1	166.835	173.332	440.836
do2	118.026	297.246	533.831
do3	68.115	163.24	437.625
do4	83.3356	105.41	447.818
do5	242.966	333.115	408.995

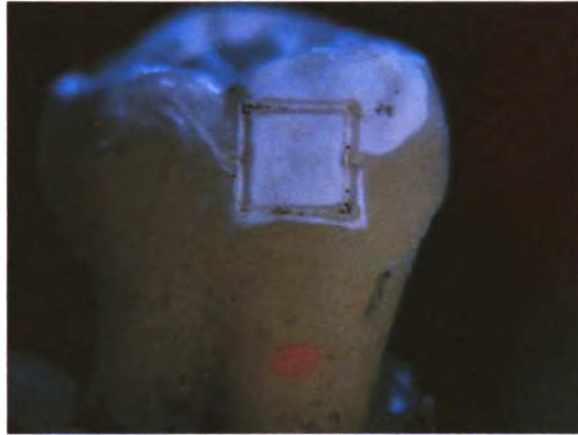
The OCT images show that there are lesions in the areas of demineralization, and that there are no lesions in the area of nail polish and sound enamel.

CONCLUSION

We found that NIR can measure contrast between sound and early caries lesion. Both clear varnish and optical adhesive do not change the optical properties of the tooth surface and is not changed optically by demineralization. Therefore, both clear varnish and optical adhesive can be used as a reference background and do not need to be removed prior to imaging.

Appendix B: Buccal images

Tooth 1



Visible with polarization



Reflective NIR with polarization



NIR Single fiber probe



NIR Transillumination



QLF

Tooth 2



Visible with polarization



Reflective NIR with polarization



Single fiber probe

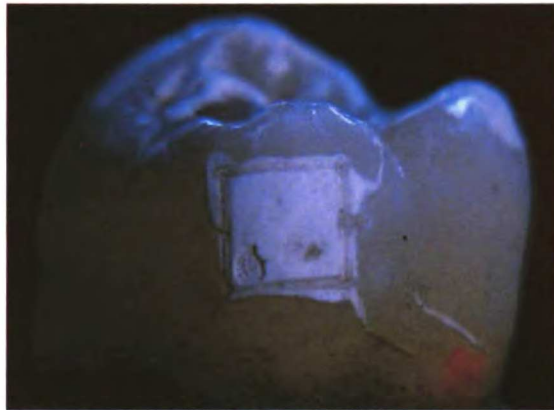


NIR Transillumination



QLF

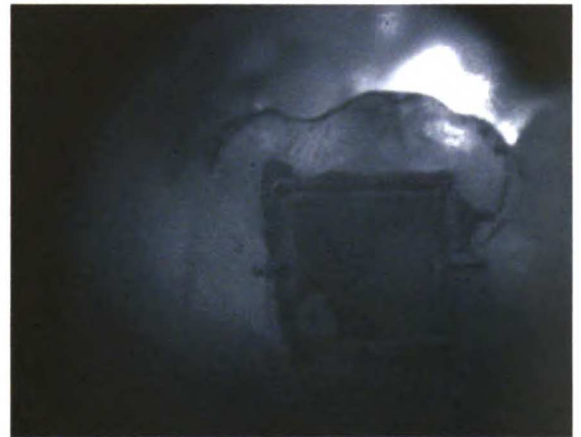
Tooth 3



Visible with polarization



Reflective NIR with polarization



NIR Single fiber probe



NIR Transillumination

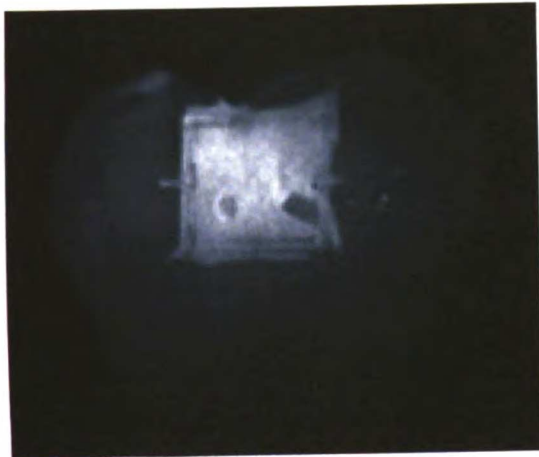


QLF

Tooth 4



Visible with polarization



Reflective NIR with polarization



NIR Single fiber probe

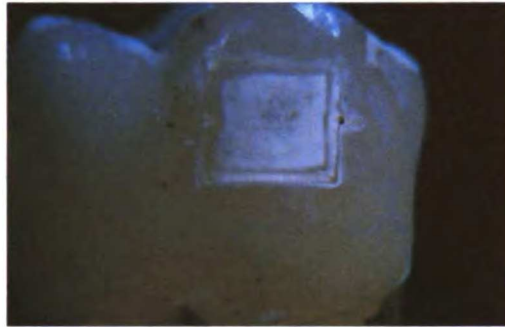


NIR Transillumination

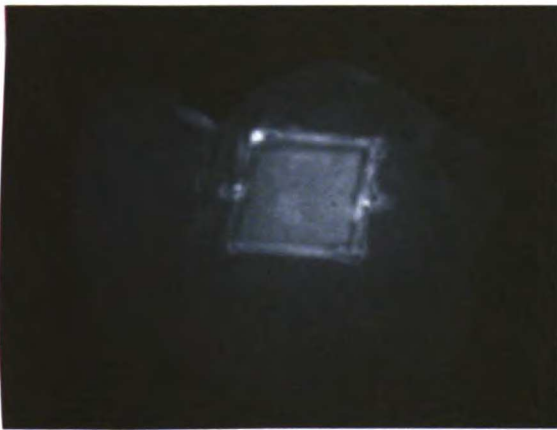


QLF

Tooth 5



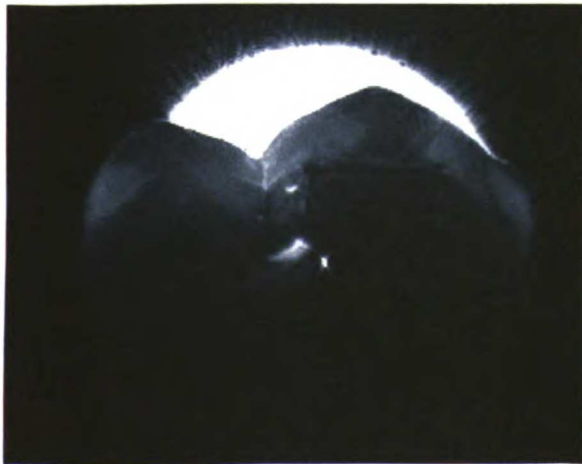
Visible with polarization



Reflective NIR with polarization



NIR Single fiber probe

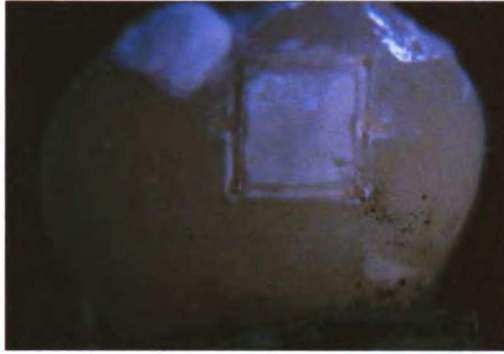


NIR Transillumination



QLF

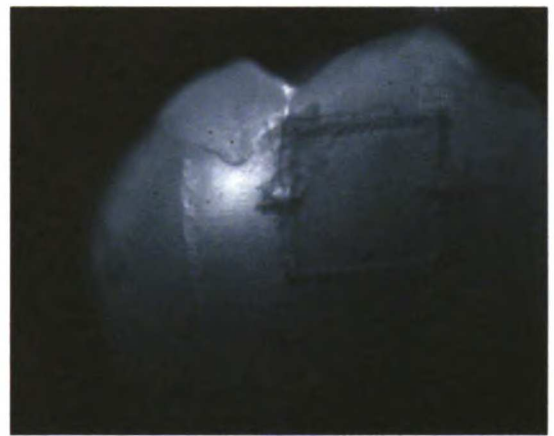
Tooth 6



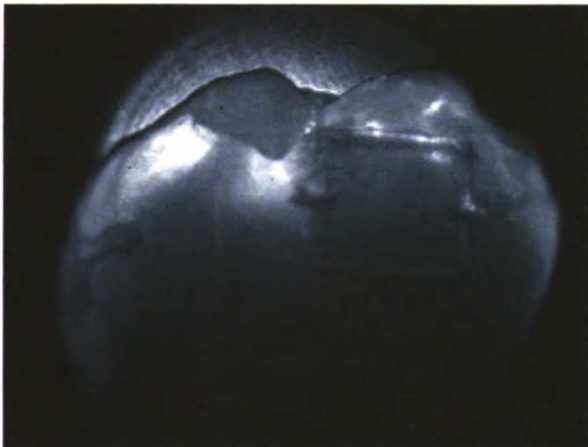
Visible with polarization



Reflective NIR with polarization



NIR Single fiber probe

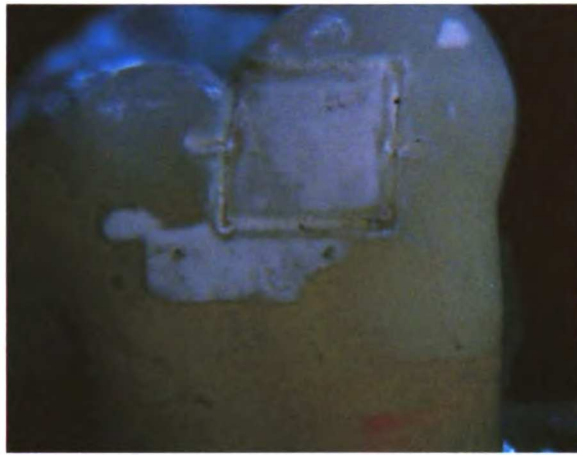


NIR Transillumination



QLF

Tooth 7



Visible with polarization



Reflective NIR with polarization



NIR Single fiber probe



NIR Transillumination

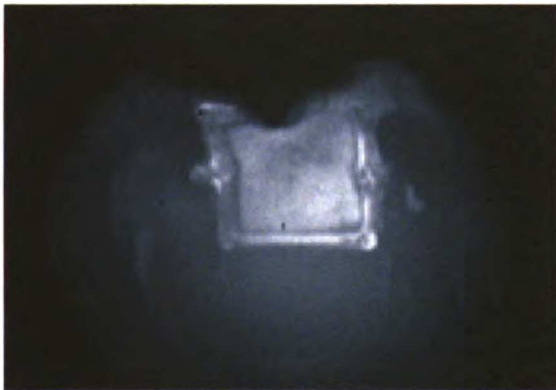


QLF

Tooth 8



Visible with polarization



Reflective NIR with polarization



NIR Single fiber probe

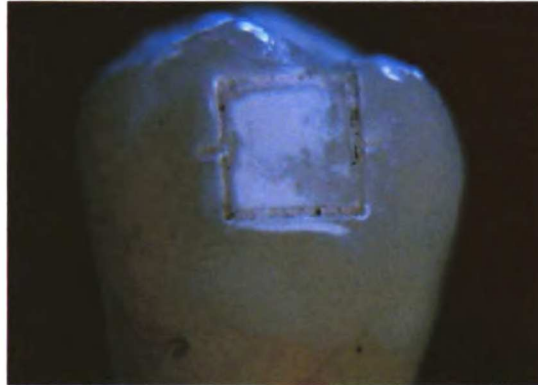


NIR Transillumination

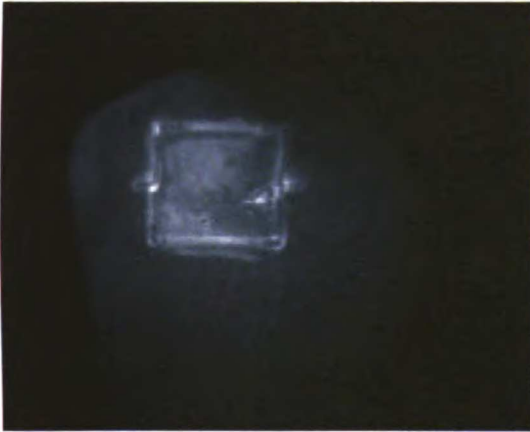


QLF

Tooth 9



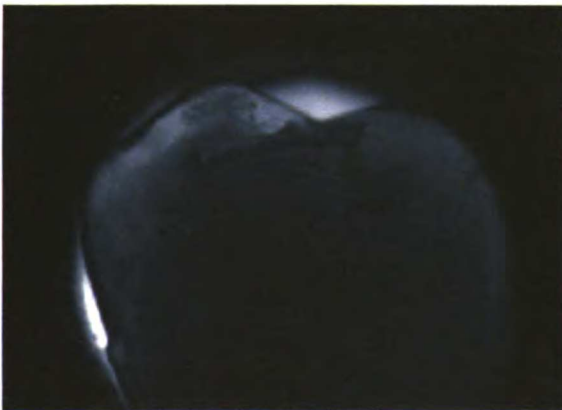
Visible with polarization



Reflective NIR with polarization



NIR Single fiber probe

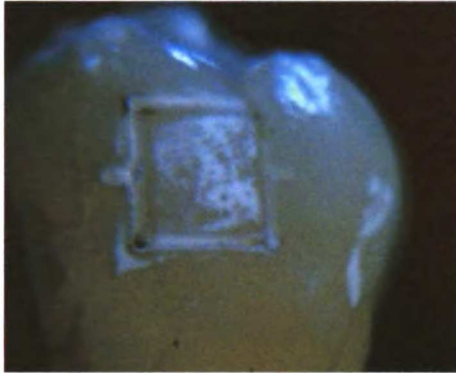


NIR Transillumination

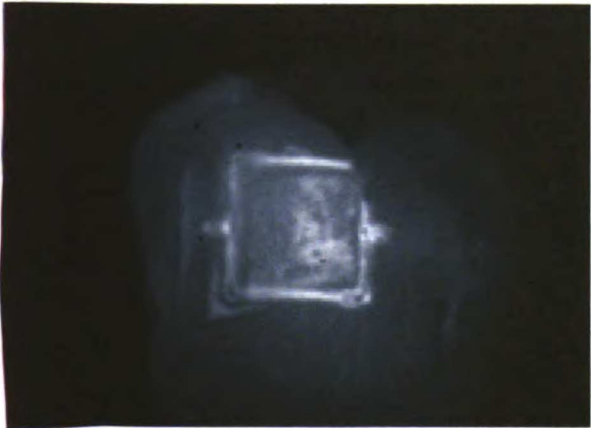


QLF

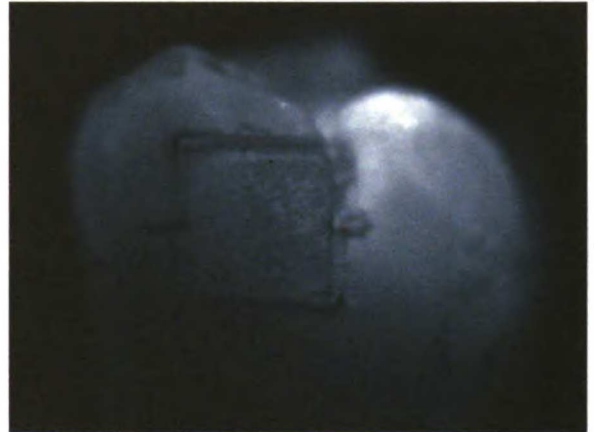
Tooth 10



Visible with polarization



Reflective NIR with polarization



NIR Single fiber probe

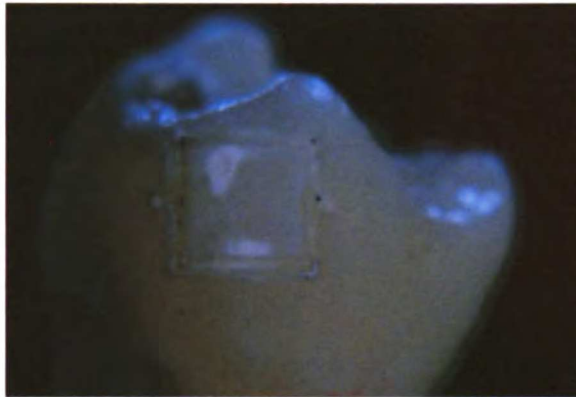


NIR Transillumination



QLF

Tooth 11



Visible with polarization



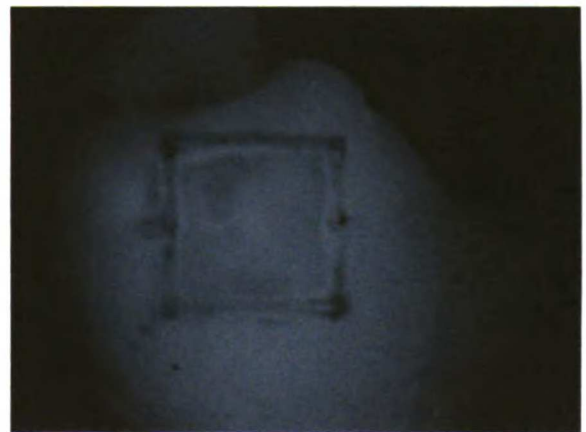
Reflective NIR with polarization



NIR Single fiber probe

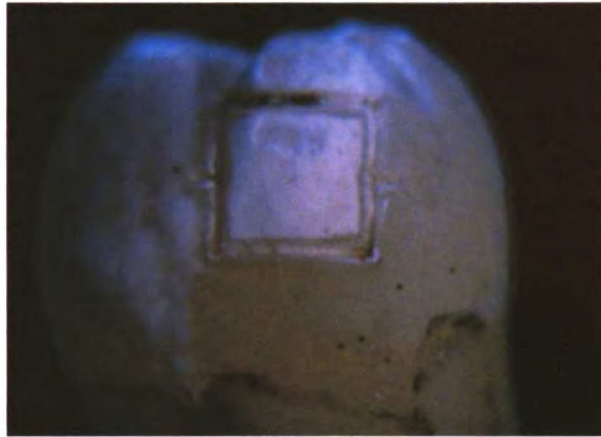


NIR Transillumination



QLF

Tooth 12



Visible with polarization



Reflective NIR with polarization



NIR Single fiber probe

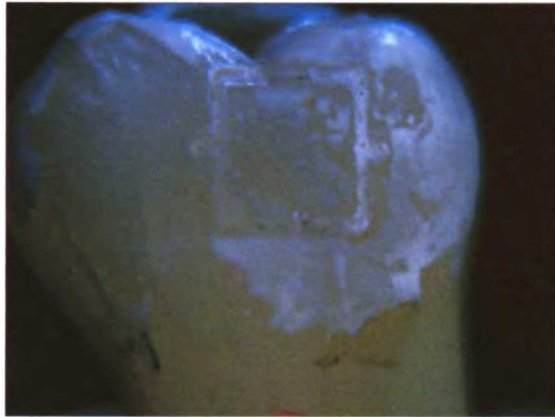


NIR Transillumination

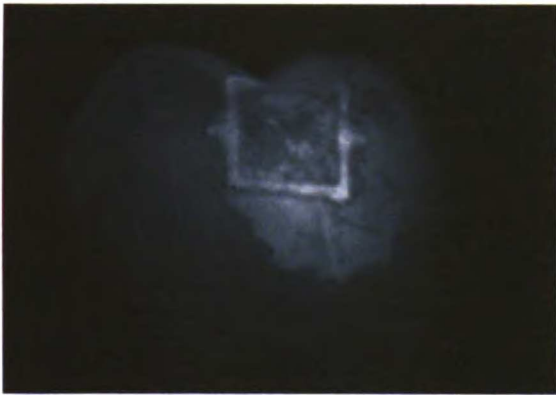


QLF

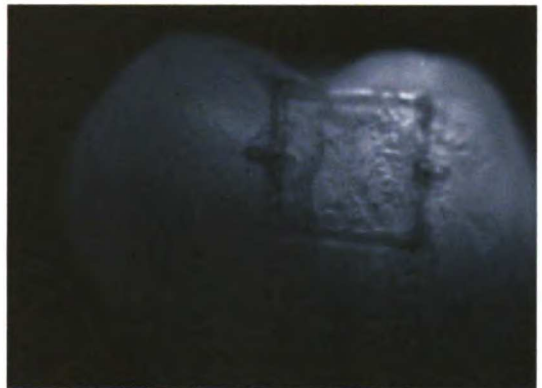
Tooth 13



Visible with polarization



Reflective NIR with polarization



NIR Single fiber probe



NIR Transillumination



QLF

Tooth 14



Visible with polarization



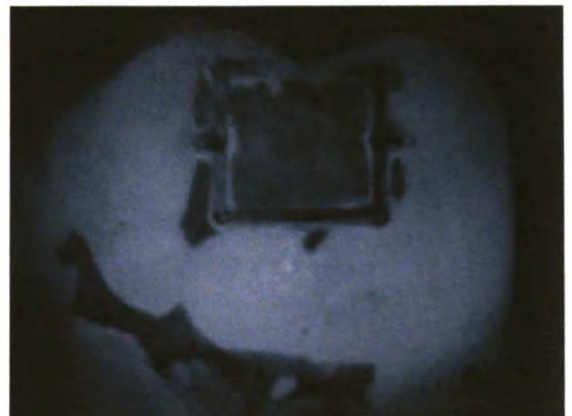
Reflective NIR with polarization



NIR Single fiber probe



NIR Transillumination

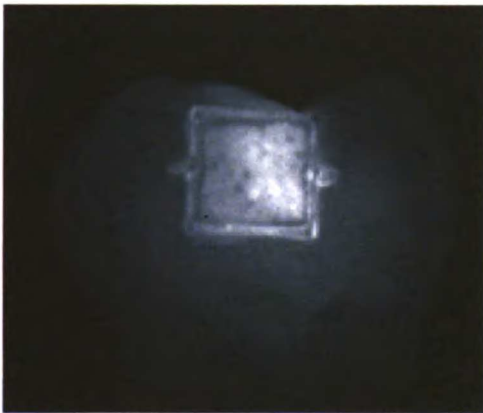


QLF

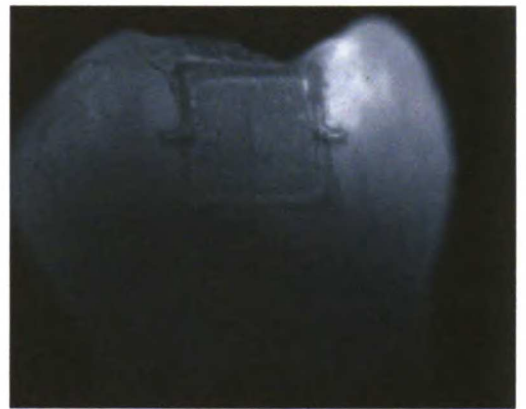
Tooth 15



Visible with polarization



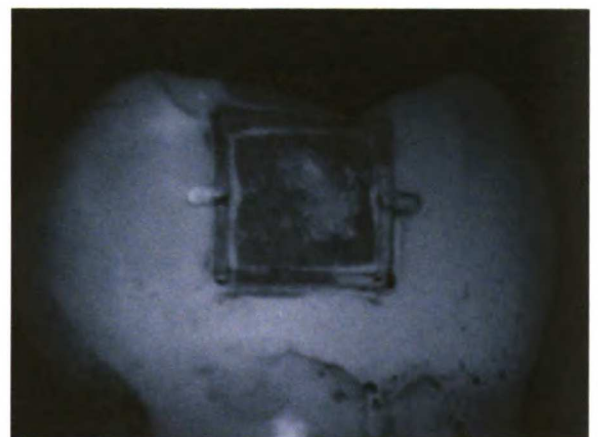
Reflective NIR with polarization



NIR Single fiber probe



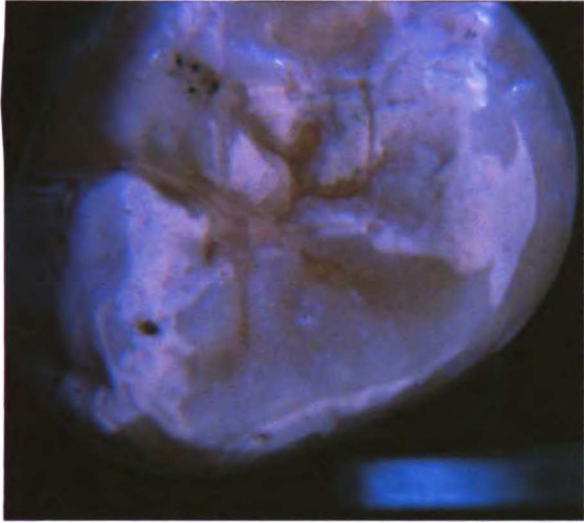
NIR Transillumination



QLF

Appendix C: Occlusal Images

Tooth1



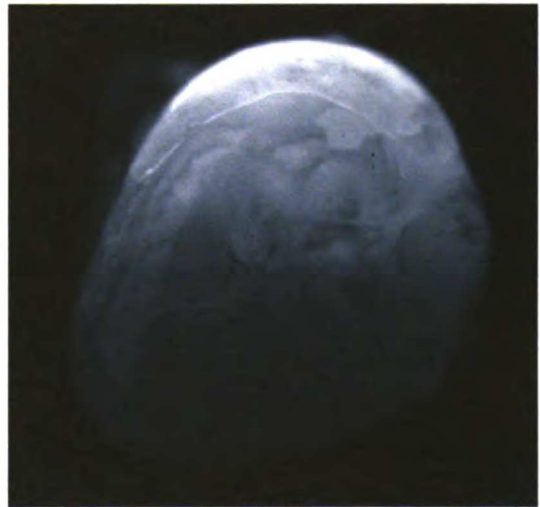
Visible with polarization



QLF

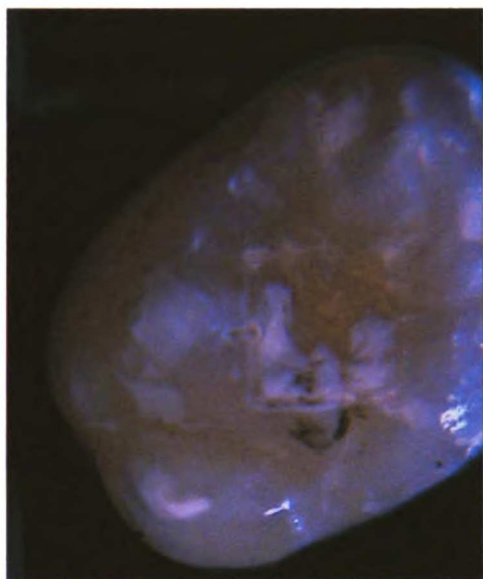


Reflective NIR with polarization



NIR Transillumination with polarization

Tooth 2



Visible with polarization



QLF

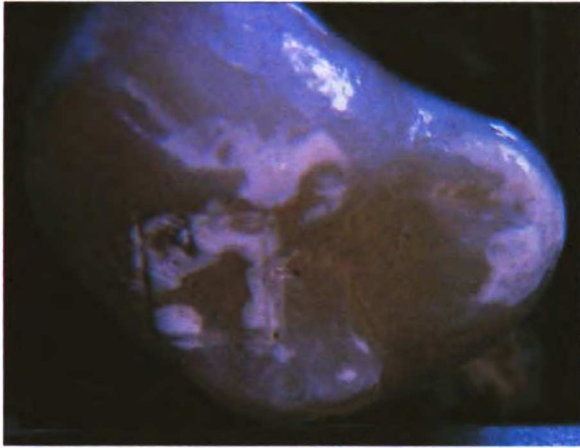


Reflective NIR with polarization



NIR Transillumination with polarization

Tooth 3



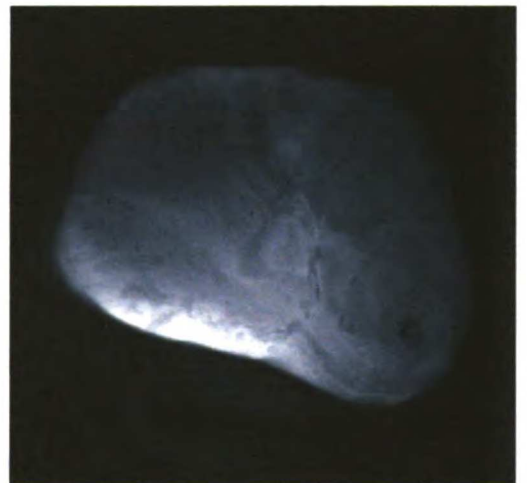
Visible with polarization



QLF



Reflective NIR with polarization

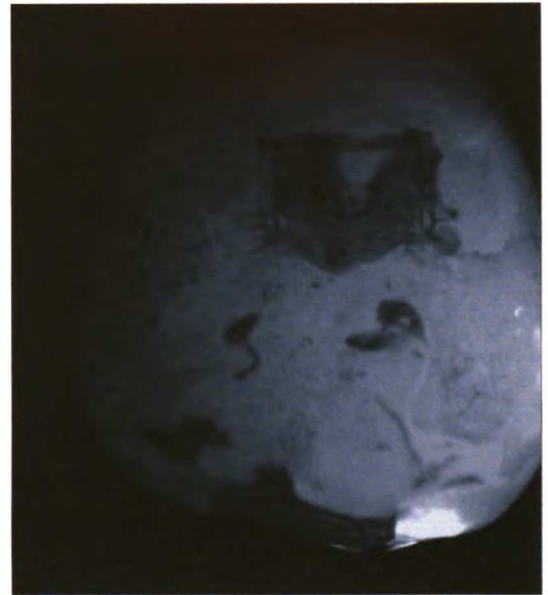


NIR Transillumination with polarization

Tooth 4



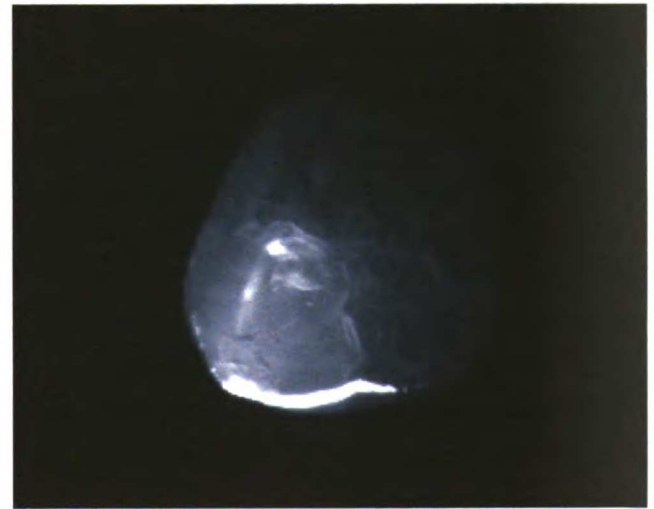
Visible with polarization



QLF

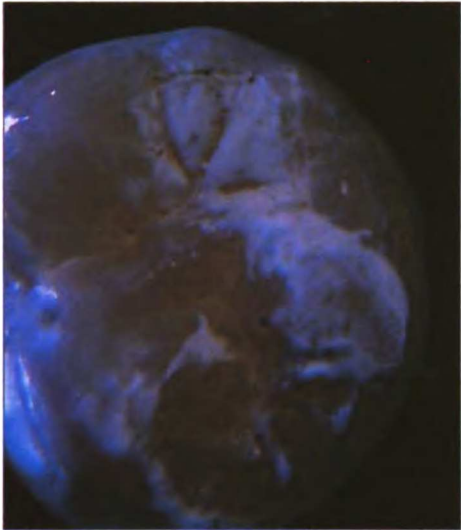


Reflective NIR with polarization



NIR Transillumination with polarization

Tooth 5



Visible with polarization



QLF

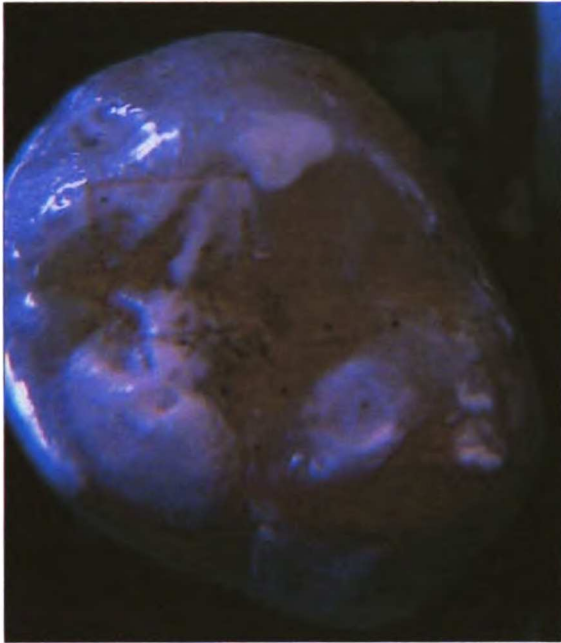


Reflective NIR with polarization



NIR Transillumination with polarization

Tooth 6



Visible with polarization



QLF

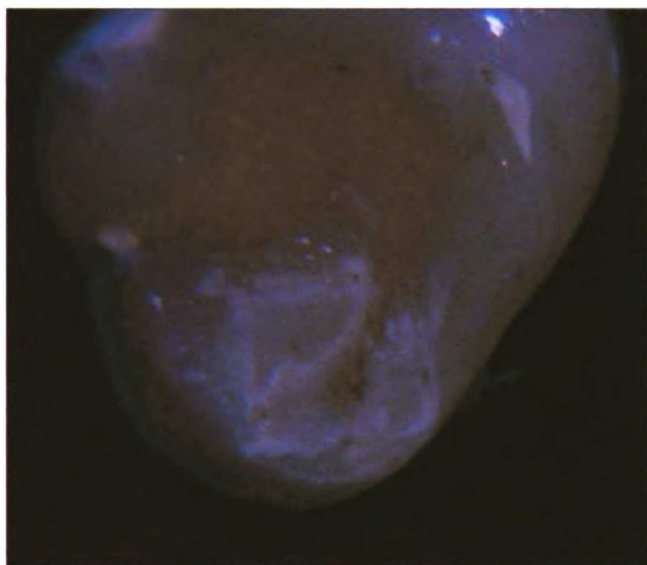


Reflective NIR with polarization

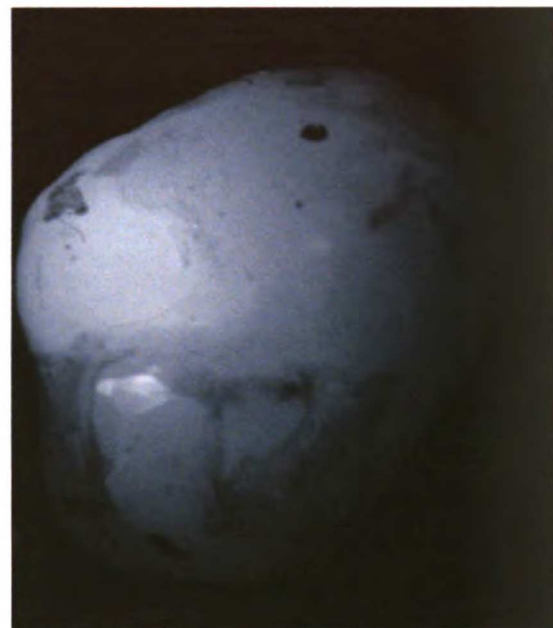


NIR Transillumination with polarization

Tooth 7



Visible with polarization



QLF

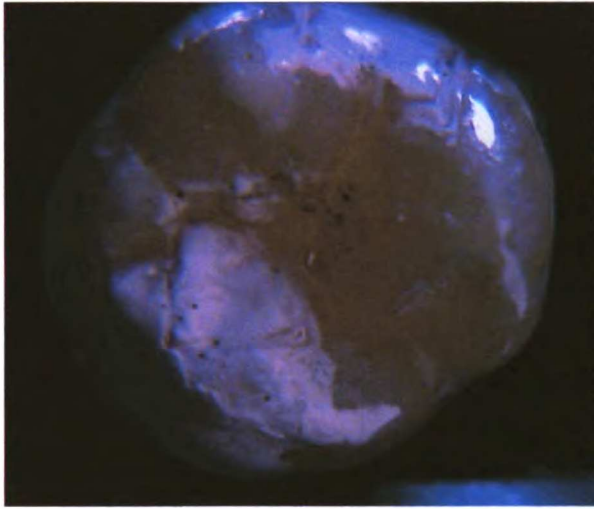


Reflective NIR with polarization

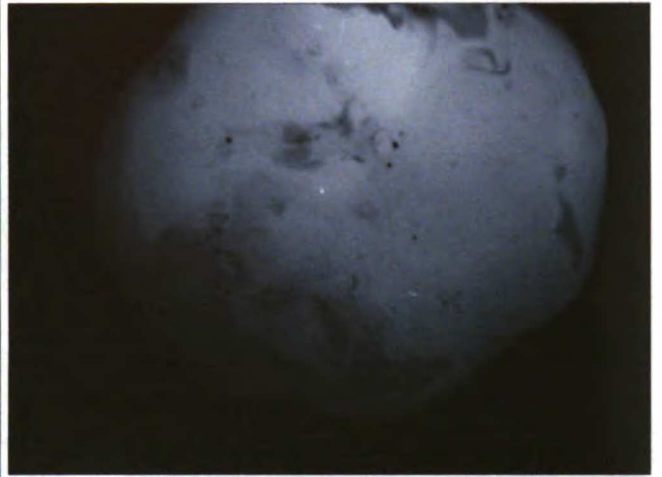


NIR Transillumination with polarization

Tooth 8



Visible with polarization



QLF

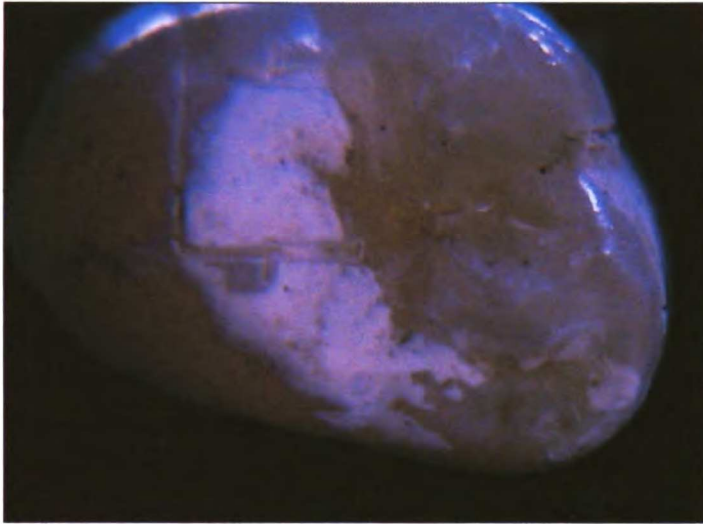


Reflective NIR with polarization

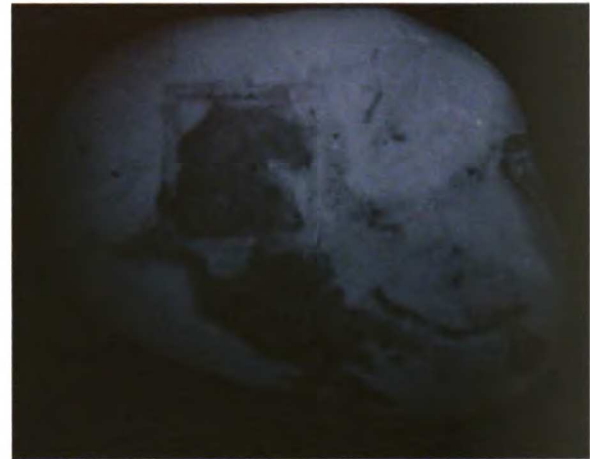


NIR Transillumination with polarization

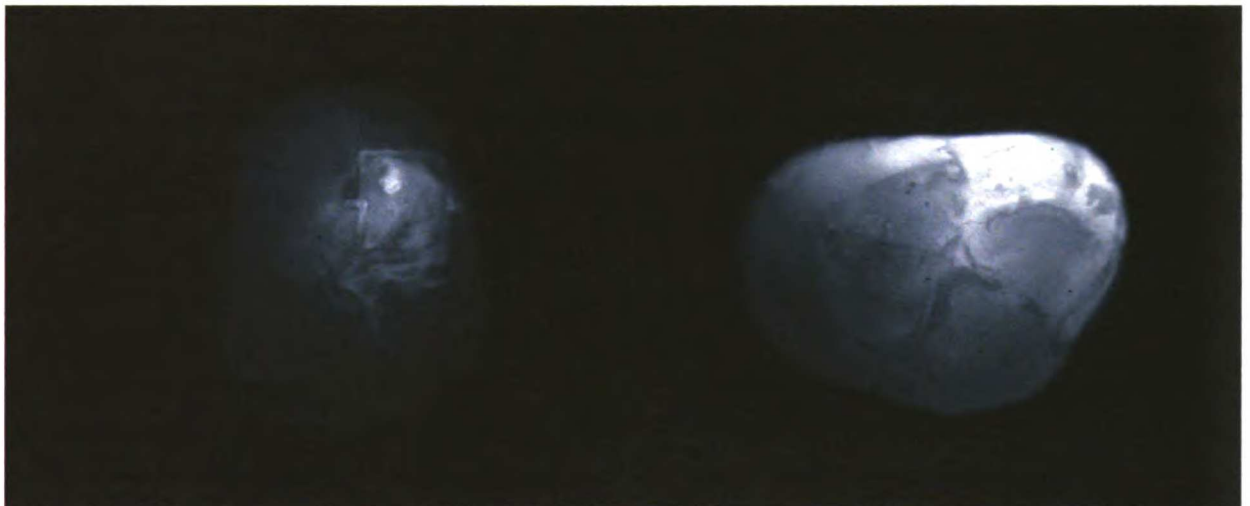
Tooth 9



Visible with polarization



QLF



Reflective NIR with polarization

NIR Transillumination with polarization

Tooth 10



Visible with polarization



QLF

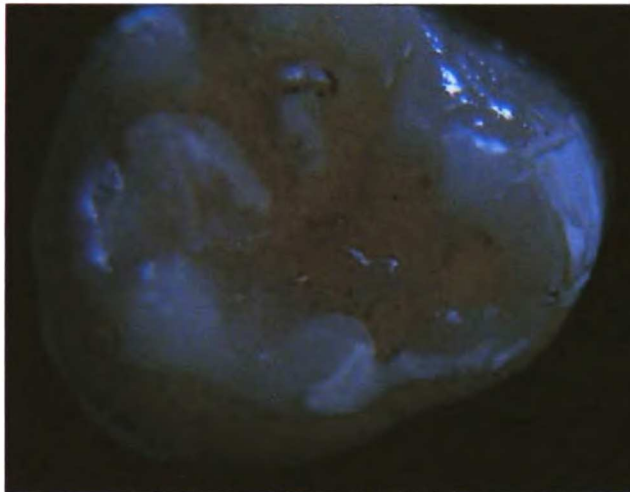


Reflective NIR with polarization



NIR Transillumination with polarization

Tooth 11



Visible with polarization



QLF



Reflective NIR with polarization



NIR Transillumination with polarization

Tooth 12



Visible with polarization



QLF



Reflective NIR with polarization

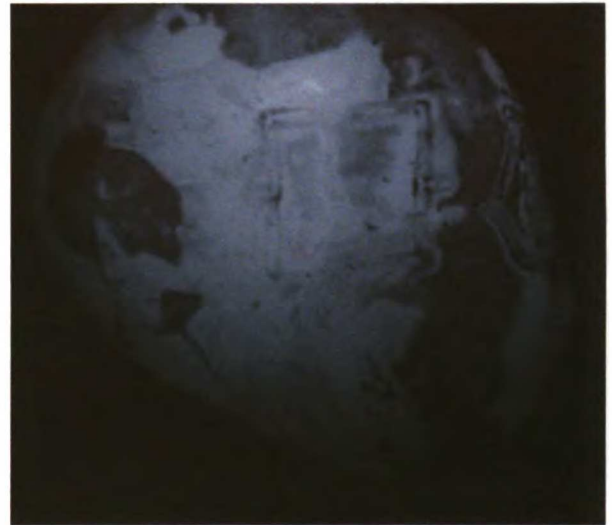


NIR Transillumination with polarization

Tooth 13



Visible with polarization



QLF



Reflective NIR with polarization



NIR Transillumination with polarization

Tooth 14



Visible with polarization



QLF

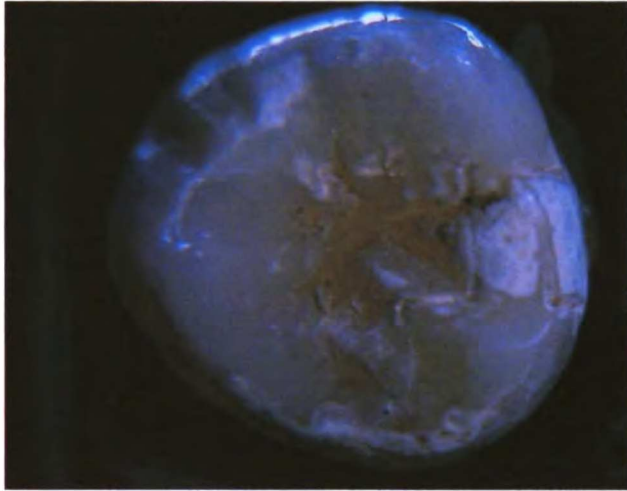


Reflective NIR with polarization



NIR Transillumination with polarization

Tooth 15



Visible with polarization



QLF



Reflective NIR with polarization



NIR Transillumination with polarization



7075651



3 1378 00707 5651

LIBRARY
USE ONLY

